PALAIOS
Emphasizing the impact of life on Earth's history

PALAIOS, 2024, v. 39, 444–461
Research Article
DOI: http://dx.doi.org/10.2110/palo.2024.007

MORPHOLOGY AND PRESERVATION OF *GAOJIASHANIA*, AN ENIGMATIC TUBULAR FOSSIL FROM THE UPPER EDIACARAN DUNFEE MEMBER, DEEP SPRING FORMATION, NEVADA, USA

ASHLEY RIVAS,[1] PAUL M. MYROW,[2] EMILY F. SMITH,[3] LYLE L. NELSON,[4,5] DEREK E.G. BRIGGS,[1,6] AND LIDYA G. TARHAN[1,6]
[1]*Department of Earth and Planetary Sciences, Yale University, New Haven, Connecticut 06520, USA*
[2]*Department of Geology, Colorado College, Colorado Springs, Colorado 80903, USA*
[3]*Department of Earth and Planetary Sciences, Johns Hopkins University, Baltimore, Maryland 21210, USA*
[4]*Department of Earth Sciences, Carleton University, Ottawa, Ontario, K1S 5B6, Canada*
[5]*Department of Earth, Atmospheric, and Planetary Sciences, Massachusetts Institute of Technology, Cambridge, Massachusetts 02139, USA*
[6]*Yale Peabody Museum, New Haven, Connecticut 06520, USA*
email: ashley.rivas@yale.edu

ABSTRACT: **The upper Ediacaran stratigraphic record hosts fossil assemblages of Earth's earliest communities of complex, macroscopic, multicellular life. Tubular fossils are a common and diverse, though frequently under-characterized, component of many of these assemblages. *Gaojiashania cyclus* is an enigmatic tubular fossil and candidate index fossil found in upper Ediacaran strata globally and is best known from the Gaojiashan Lagerstätte of South China. Here we describe a recently discovered assemblage of *Gaojiashania* fossils from the Ediacaran Dunfee Member of the Deep Spring Formation of Nevada, USA. Both body and trace fossil affinities have been proposed for *Gaojiashania*; we present morphological and biostratinomic evidence for a body fossil affinity for the Dunfee specimens. Additionally, previous studies have highlighted that Ediacaran tubular fossils are characterized by a wide range of preservational modes, including association with pyrite, apatite, or clay minerals and preservation as carbonaceous compressions. Petrographic, SEM, and EDS data indicate that the Dunfee *Gaojiashania* specimens are preserved as 'Ediacara-style' external, internal and composite molds, in siltstone and sandstone with a clay mineral-rich matrix of both aluminosilicates and non-aluminous Mg- and Fe-rich silicate minerals that we interpret as authigenic clays. Authigenic clay-mediated fossilization of unmineralized tissues, including moldic preservation in heterolithic siliciclastic strata, as indicated by the Dunfee *Gaojiashania*, may be linked to the prevalence of both silica-rich and ferruginous seawater conditions prior to both the radiation of silica-biomineralizing organisms and the rise of ocean and atmospheric oxygen to modern levels. In this light, clay authigenesis may have played a critical role in facilitating multiple modes of Ediacaran and Cambrian exceptional fossilization, thus shaping the stratigraphic distribution of a range of Ediacara macrofossil taxa.**

INTRODUCTION

The Ediacara Biota provides the earliest fossil record of multicellular macroorganisms in morphologically and ecologically complex communities (Narbonne 2005; Xiao and Laflamme 2009). Although fossils of biomineralizing macroorganisms are present in uppermost Ediacaran strata, most Ediacaran taxa—including those of the Ediacara Biota—were entirely soft-bodied. Ediacara Biota macrofossils are globally distributed and predominantly occur as sandstone casts and molds (e.g., Wade 1968; Seilacher et al. 1985; Seilacher 1989; Gehling 1999; Narbonne 2005), in what has been termed "Ediacara-style" preservation (Tarhan et al. 2016). Ediacara fossil assemblages record a number of evolutionary and ecological innovations, including features and behaviors characteristic of modern animal communities (Clapham and Narbonne 2002; Rogov et al. 2012; Mitchell et al. 2015; Droser et al. 2017; Tarhan et al. 2018).

The term "tubular fossil" has been applied to a wide range of Ediacaran macrofossils with tube-shaped morphologies, including tubiform, cloudinomorph, conotubular, and ovatubular body plans (Surprenant et al. 2024). Individual taxa are further distinguished on the basis of size and aspect ratio, cross-sectional geometry and the presence of annuli, among other features. Tubular fossils are present in upper Ediacaran strata worldwide, including well-documented Ediacara Biota-hosting deposits of the White Sea and Nama Assemblages (e.g., Schiffbauer et al. 2016; Droser et al. 2017; Darroch et al. 2021) as well as other Ediacaran successions (e.g., Jensen 2003). Ediacaran tubular fossils are preserved in a variety of different taphonomic modes, including calcified, pyritized, replaced by clay minerals, as carbonaceous compressions, and moldically in a manner typical of Ediacara-style fossils (e.g., Cai et al. 2010; Tarhan et al. 2018). Assemblages of tubular taxa include *Conotubus*, *Cloudina*, *Gaojiashania*, *Shaanxilithes*, and *Sinotubulites* in the Gaojiashan Lagerstätte of South China (Cai et al. 2010, 2011b, 2012, 2013, 2014; An et al. 2020); *Cloudina*, *Corumbella*, *Gaojiashania*, *Shaanxilithes*, *Vendotaenia*, and other taxa in the Nama Group of Namibia (e.g., Cohen et al. 2009; Penny et al. 2014; Darroch et al. 2016; Elliott et al. 2016; Smith et al. 2017; Turk et al. 2022); *Shaanxilithes* in the Krol and Tal groups in India (Tarhan et al. 2014); *Cloudina*, *Costatubus*, *Corumbella*, *Gaojiashania*, *Saarina, Sinotubulites*, and other non-mineralized cloudinomorphs in the Death Valley, White–Inyo, and Carborca regions of southwestern North America (Signor et al. 1987; Hagadorn and Waggoner 2000; Sour-Tovar et al. 2007; Smith et al. 2017; Schiffbauer et al. 2020; Selly et al. 2020; Hodgin et al. 2021); *Aulozoon*, *Funisia*, *Plexus*, and *Somatohelix* in the

Published Online: December 2024
 0883-1351/24/039-444

Ediacara Member of South Australia (e.g., Droser and Gehling 2008; Sappenfield et al. 2011; Joel et al. 2014; Droser et al. 2017; Surprenant et al. 2020; Surprenant and Droser 2024; and *Cloudina* and other cloudinids from the Ibor Group in Spain (Cortijo et al. 2010) and elsewhere. The abundance, diversity, and paleogeographic range of tubular fossils indicate that these organisms likely contributed substantially to the diversity and ecology of late Ediacaran seafloor communities.

Ediacaran tubular fossils have been subject to a range of anatomical, ecological, and phylogenetic interpretations (e.g., Hua et al. 2005; Vinn and Zaton 2012; Mehra and Maloof 2018; Schiffbauer et al. 2020; Yang et al. 2020). Recent work has suggested, based on both detailed morphological study and the presence of similar body plans among modern organisms of disparate affinities, that they likely represent a polyphyletic group, which may include organisms of poriferan, cnidarian, bilaterian or even macroalgal affinity (e.g., Tarhan et al. 2018; Selly et al. 2020). Although most Ediacaran tubular organisms appear to have been entirely soft-bodied, Ediacaran tubular taxa provide some of the earliest evidence for partial or full biomineralization, including the nested funnel-in-funnel fossil *Cloudina* and other cloudinomorphs (Germs 1972; Grant 1990; Yue et al. 1992; Amthor et al. 2003; Hua et al. 2005; Chen et al. 2008; Cortijo et al. 2010, 2015a, 2015b; Cai et al. 2011b, 2014, 2015, 2017; Wood et al. 2017; Wood 2018; Selly et al. 2020; Yang et al. 2020), as well as the corrugated and variably triradial, pentaradial, and hexaradial *Sinotubulites* (Cai et al. 2015). Soft-bodied tubular taxa, however, have received relatively less scrutiny than either biomineralizing tubular taxa or more 'classic' Ediacara Biota macrofossil taxa—due in part to the historical conflation of non-biomineralizing tubular fossils with trace fossils and other sedimentary features, and limited insight into their taphonomy (e.g., Jensen 2003). Nonetheless, these soft-bodied tubular taxa may also record distinct anatomies, autecologies, and taphonomic histories. Therefore, study of soft-bodied tubular taxa may shed critical light on late Ediacaran seafloor ecology and environmental conditions that shaped the lives, deaths, and fossilization of members of these assemblages, as well as the dramatic taxonomic turnover associated with the Ediacaran–Cambrian transition (Seilacher et al. 2005; Laflamme et al. 2013; Darroch et al. 2023). Additionally, several biomineralizing and non-biomineralizing tubular taxa—foremost *Cloudina*, *Shaanxilithes*, and *Gaojiashania*—have been proposed as potential index fossils for the upper Ediacaran (e.g., Grant 1990; Narbonne et al. 2012; Cai et al. 2015, 2017; Xiao et al. 2016). A clear understanding of the paleoenvironmental distribution and taphonomic pathways responsible for the fossilization of these taxa is essential for determining the evolutionary significance of their stratigraphic ranges and their possible utility as index fossils.

Gaojiashania

Much of the available information on the morphology and preservation of *Gaojiashania* stems from characterization of the eponymous upper Ediacaran Gaojiashan Lagerstätte in the Dengying Formation of South China. Although multiple species of *Gaojiashania*, including *G. cyclus*, *G. zonatus*, *G. annulucosta*, and *G. caperata* have been described, recognition that these reflect taphonomic variants rather than species-level diversity has led to synonymization of all species to *G. cyclus*; *Gaojiashania* is currently a monospecific genus (Cai et al. 2013). *Gaojiashania* commonly co-occurs with other tubular fossils such as cloudinomorphs and *Wutubus* (e.g., in the Denying Formation of South China, Wood Canyon and Deep Spring formations of Nevada, and the Nama Group in Namibia) (Cai et al. 2010; Smith et al. 2016, 2017, 2023). In contrast to some cloudinomorphs that have been documented in lower Cambrian strata (Yang et al. 2020; Park et al. 2021), *Gaojiashania* is one of many tubular fossils that appears to be confined to the upper Ediacaran, making it a potential index fossil for the Ediacaran–Cambrian transition (Cai et al. 2010; Smith et al. 2016).

The ecology and physiology of *Gaojiashania* remain subjects of debate. *Gaojiashania* is commonly interpreted as soft-bodied or lightly mineralized (Cai et al. 2013). The tube consists of annuli, usually uniformly spaced, that are separated by larger rings. The arrangement of annuli has been used to infer modes of growth and reproduction, e.g., curving, extension, or constriction of the rings may reflect different angles of growth (Cai et al. 2013). Due in large part to the lack of an associated holdfast, *Gaojiashania* has been commonly reconstructed in a life position prone on the seafloor (Cai et al. 2013). Specimens of *Gaojiashania* in the Gaojiashan Lagerstätte are primarily preserved through pyritization (e.g., Cai et al. 2010), although they are also preserved via replacement by clay minerals such as glauconite (Cai et al. 2010, 2012). Clay minerals have been associated with Burgess Shale-type carbonaceous preservation of soft tissues (e.g., Anderson et al. 2018) and glauconite-replaced shelly fossils have also been described from Cambrian strata (Pruss et al. 2019). Non-pyritized *Gaojiashania* are most commonly preserved as either two-dimensional clay compressions or as casts and molds (e.g., this study) but specimens preserved as combined carbonaceous and clay compressions have also been documented (Cai et al. 2012).

Fossils attributed to *Gaojiashania* previously have been recovered from both the Ediacaran Dunfee Member of the Deep Spring Formation and the lower member of the Wood Canyon Formation of Nevada, where they occur in a variety of taphonomic modes, including moldic Ediacara-style preservation, as possible clay compressions, and replaced by pyrite. Here we describe the morphology and taphonomy of moldically preserved *Gaojiashania* from the Deep Spring Formation of Nevada (see Smith et al. 2016, 2023) and propose a new model for the fossilization of this assemblage. These data provide new insights into the depositional conditions and diagenetic pathways that fostered the exceptional fossilization of early complex macroorganisms in late Ediacaran shallow seafloor settings.

GEOLOGIC SETTING

Upper Neoproterozoic–lower Paleozoic strata that were deposited along the northwest-facing margin of southwestern Laurentia are preserved in the White-Inyo Ranges and the Death Valley region of California and adjacent Esmeralda County of Nevada (Nelson 1962; Stewart et al. 1966; Smith et al. 2023). This region has undergone significant tectonic deformation, including late Paleozoic and Mesozoic contraction and metamorphism, and Cenozoic metamorphism (e.g., Morgan and Law 1998) and trans-tensional brittle deformation (e.g., Wernicke et al. 1988). Relative to other Neoproterozoic and lower Paleozoic successions of the southern Great Basin, the strata in Esmeralda County have been interpreted as some of the most distal preserved deposits (e.g., Smith et al. 2023).

The Deep Spring Formation at Mount Dunfee, near Gold Point, NV, consists of $\sim$ 700 m of interbedded limestone, siltstone, and sandstone (Fig. 1; Stewart 1970; Corsetti and Hagadorn 2003; Smith et al. 2023). The Deep Spring Formation overlies the Reed Dolomite and consists, in stratigraphic order, of the Dunfee, Esmeralda, and Gold Point members (Fig. 1). The Dunfee Member, from which *Gaojiashania* specimens were recovered, is characterized by thinly interbedded heterolithic strata with mudstone intraclasts, mud cracks, and syneresis cracks. This facies is interbedded with tabular and hummocky cross-stratified, tool-marked sandstone and carbonate grainstone (Fig. 2). The facies of the lower Dunfee Member record a range of shallow marine depositional environments along a mixed carbonate-siliciclastic ramp, from nearshore and peritidal to proximal offshore settings, including storm-influenced, high-energy shoreface to transition-zone (inner shelf) environments (Corsetti and Hagadorn 2003; Tarhan et al. 2020; Smith et al. 2023).

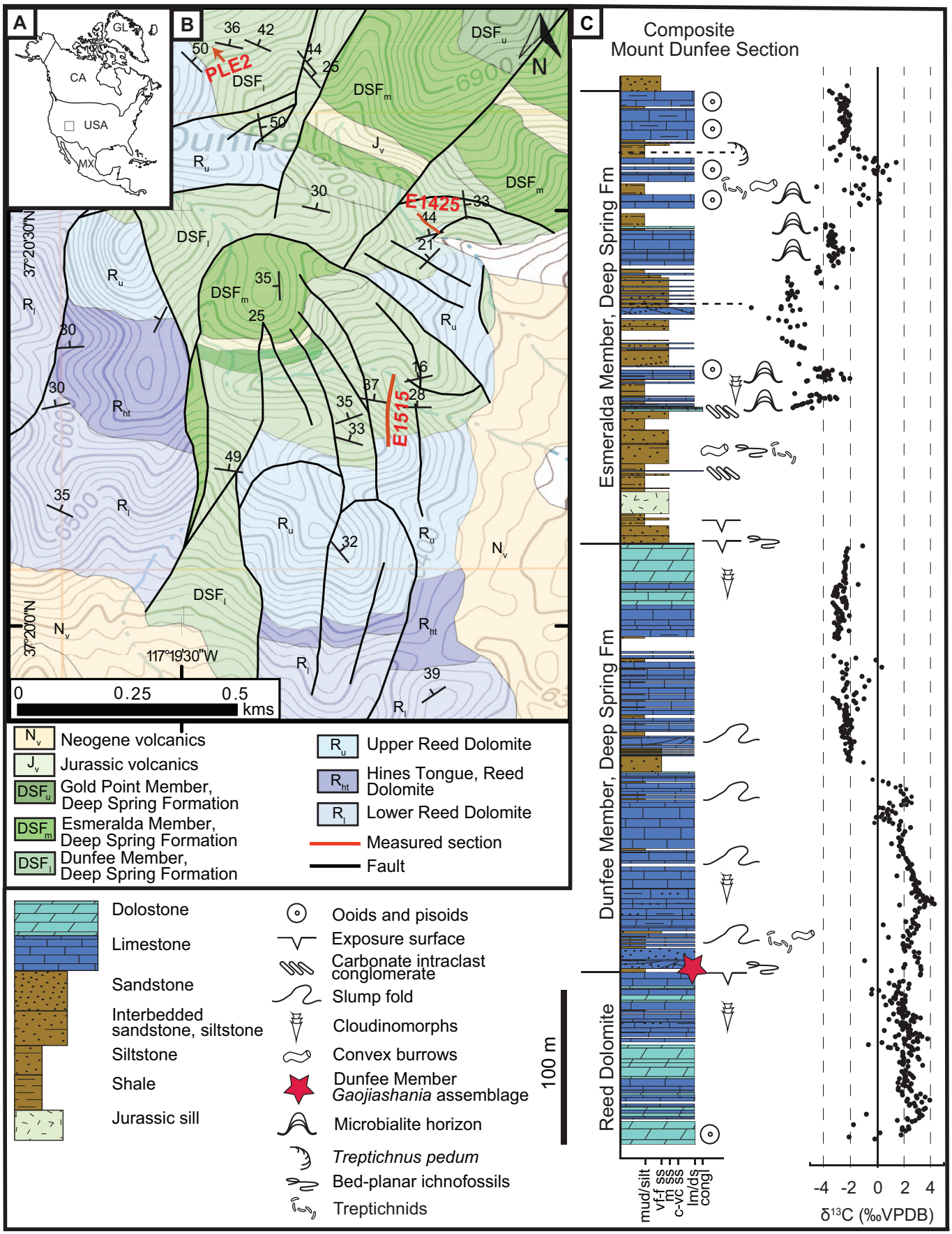

←

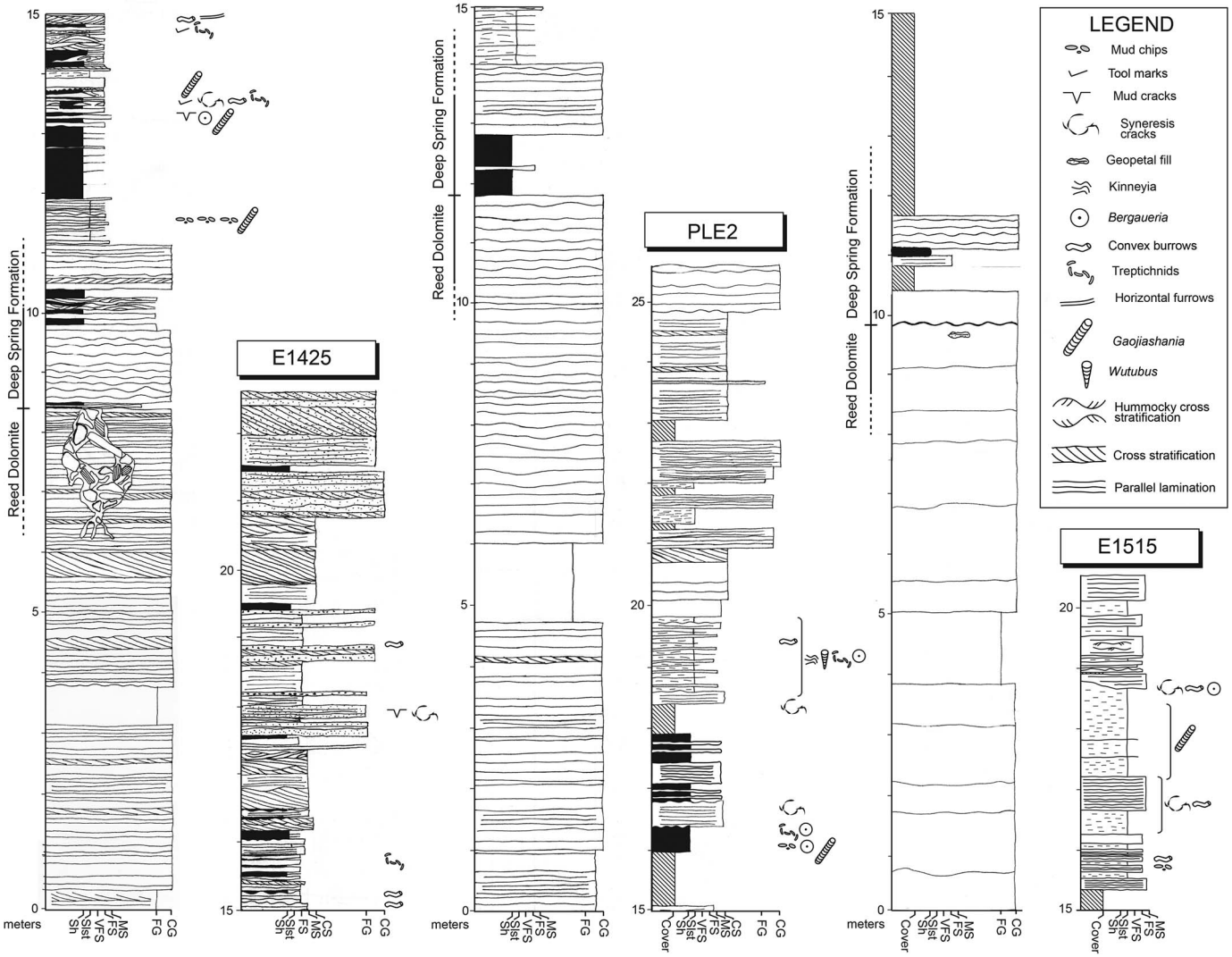

FIG. 2.—Detailed lithostratigraphy and fossil occurrences for the uppermost Reed Dolomite and lower Dunfee Member, Deep Spring Formation at Mount Dunfee as logged at fossiliferous sections E1425 (N37°20.465', W117°19.206'), PLE2 (N37°21.052', W117°19.631'), and E1515 (N37°33.659', W117°32.172'). Horizons yielding the tubular fossils *Gaojiashania* and *Wutubus* as well as trace fossils are noted. Key: Sh = shale; Slst = siltstone; VFS = very fine-grained sandstone; FS = fine-grained sandstone; MS = medium-grained sandstone; CS = coarse-grained sandstone; FG = fine grainstone; CG = coarse grainstone. Reproduced with permission from Tarhan et al. (2020).

The stratigraphic placement and geochronologic age of the Ediacaran–Cambrian boundary in this region have been estimated using a variety of methods, including carbon isotope chemostratigraphy, biostratigraphy, and detrital zircon geochronology (Hagadorn and Waggoner 2000; Corsetti and Hagadorn 2003; Smith et al. 2017; Hodgin et al. 2021; Nelson et al. 2023). A negative carbon isotope excursion recorded in the upper Esmeralda Member of the Deep Spring Formation has been proposed to correlate with the BACE (BAsal Cambrian negative carbon isotope Excursion) (Bowring et al. 1993; Grotzinger et al. 1995; Corsetti and Hagadorn 2003; Smith et al. 2016, 2023). Globally and locally, this excursion is also broadly correlated with the disappearance of Ediacara-type macrofossils and the first appearance of the complex, three-dimensional trace fossil *Treptichnus pedum*, the index fossil for the Ediacaran–Cambrian boundary (Narbonne et al. 1987; Landing 1994; Corsetti and Hagadorn 2003). Regionally, the first appearance of *T. pedum* and recovery from the BACE are estimated to have occurred no earlier than ~ 533 Ma, based on detrital

←

FIG. 1.—Geographic and stratigraphic context of units included in this study. **A**) Locality map showing the study area in western Nevada. **B**) Map showing the stratigraphic and geographic distribution of geologic units cropping out in this region; the Dunfee Member of the Deep Spring Formation is the focus of this study. **C**) Stratigraphic column of the Mount Dunfee section, including lithofacies, biostratigraphic and chemostratigraphic ($\delta^{13}C_{carbonate}$) data. The red star indicates the occurrence of *Gaojiashania*. Adapted from Smith et al. (2016) and Tarhan et al. (2020).

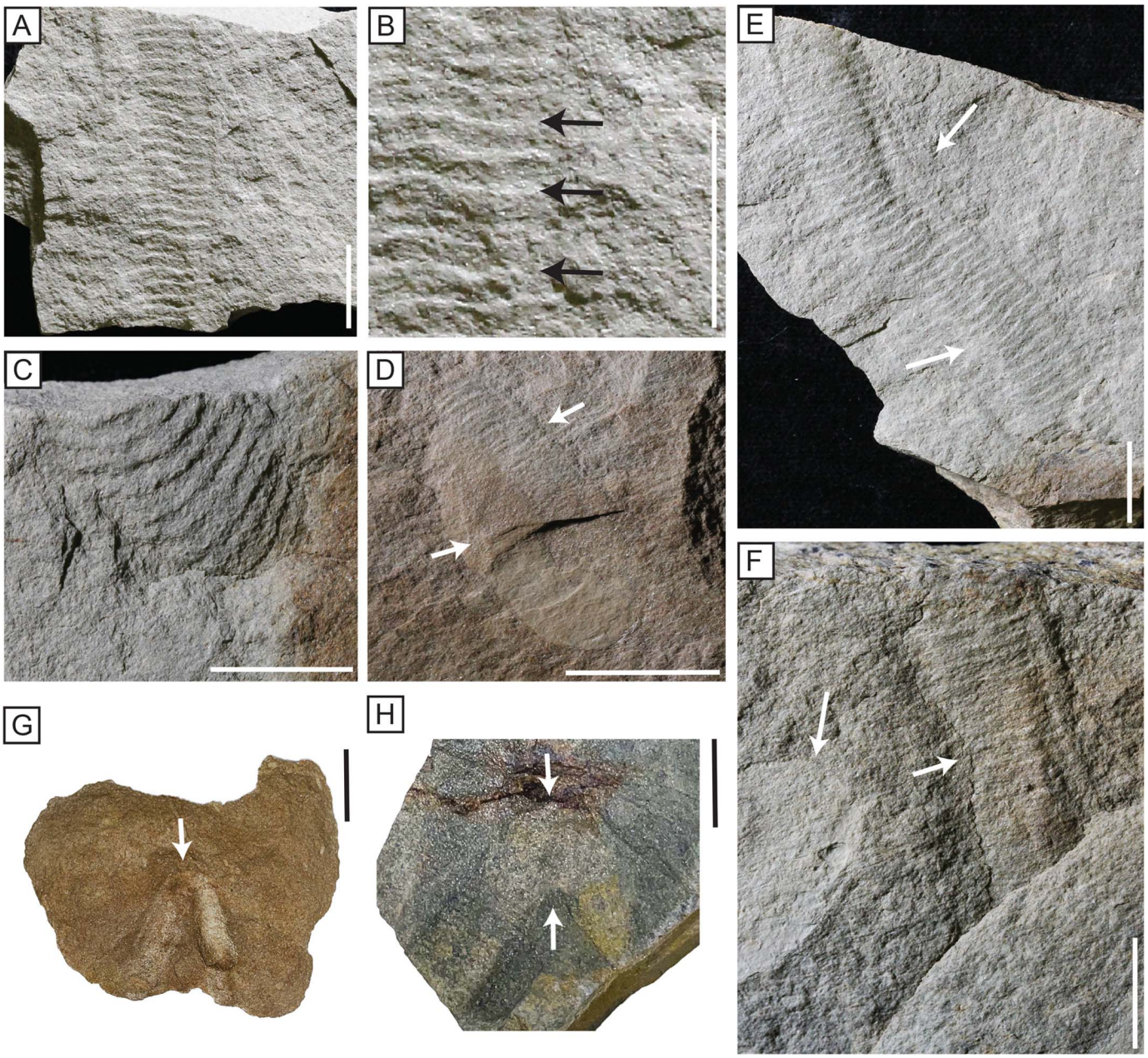

FIG. 3.—Images of *Gaojiashania* hand samples. **A**, **B**) USNM-PAL-794720, specimen of *Gaojiashania* in fine-grained sandstone, and inset of specimen shown in A, respectively. Black arrows indicate examples of rings on the tubular body with morphology characteristic of *Gaojiashania*. **C**) Sample USNM-PAL-794717 showing curvature of a *Gaojiashania* tubular body of uniform diameter. **D**) Sample USNM-PAL-974715 showing composite mold of *Gaojiashania*; fossil (right arrow) is immediately adjacent to a mudstone intraclast (left arrow) and appears to be partially infilled with light-colored mudstone. **E**) Sample USNM-PAL-794720, the counterpart of sample shown in panels A and B. White arrows indicate areas where curving of the tubular body is observed. **F**) Sample USNM-PAL-794709, containing a mudstone intraclast (left arrow) and adjacent *Gaojiashania* fossil (right arrow). Right white arrow also indicates sediment overlying the margin of *Gaojiashania*. **G**, **H**) Two samples, USNM-PAL-794726 (G) and USNM-PAL-794728 (H), where fossils are strongly overfolded or bent, as indicated by the white arrows, in siltstone and very fine-grained sandstone, respectively. Scale bars = 1 cm.

zircon geochronology of the correlative lower member of the Wood Canyon Formation (Nelson et al. 2023).

A variety of Ediacaran tubular fossils has been reported from the uppermost Reed Dolomite and the Dunfee and Esmeralda members of the Deep Spring Formation; trace fossils have also been reported from the Dunfee and Esmeralda members. Cloudinomorphs are present in the Reed Dolomite and in the Reed Dolomite–Deep Spring transition interval (Smith et al. 2023) and *Cloudina* is found in the upper part of the Dunfee Member of the Deep Spring Formation (Tarhan et al. 2020; Smith et al. 2023). Mudstones, siltstones, and fine-grained sandstones in the lower Dunfee Member contain a variety of soft-bodied tubular fossils, including specimens previously informally identified as *Gaojiashania* and *Wutubus*, as well as other problematica (Smith et al. 2016). The Esmeralda Member contains the pyritized Ediacaran cloudinomorphs *Costatubus bibendi* and *Saarina hagadorni* (Smith et al. 2016; Selly et al. 2020). Although the lowest stratigraphic occurrence of *T. pedum* is in the upper

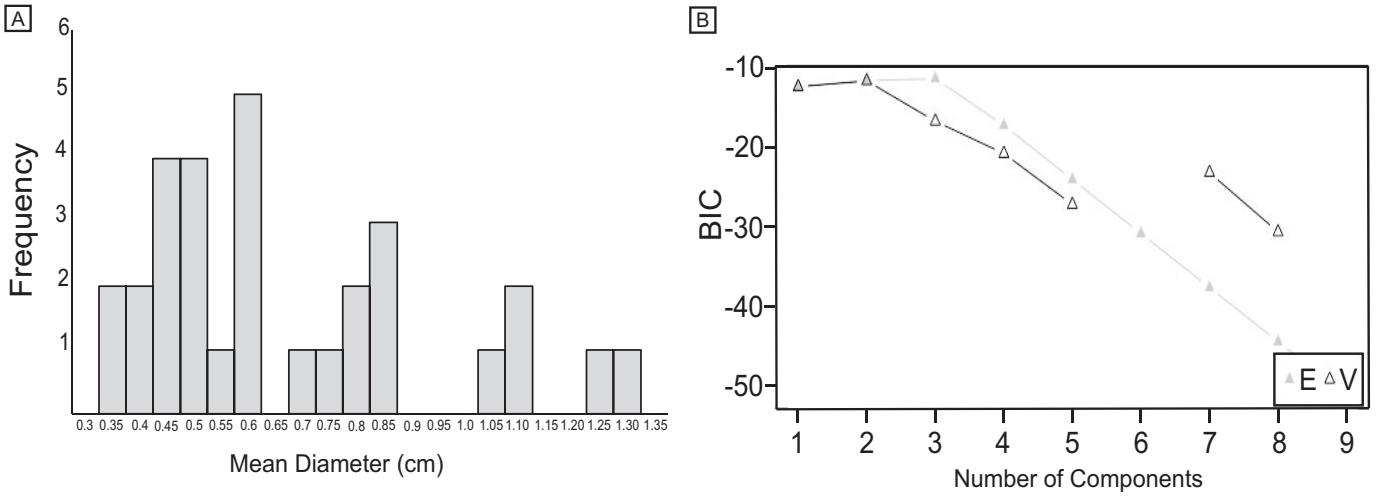

FIG. 4.—Morphometric observations and cluster analyses of the Dunfee *Gaojiashania* specimens. **A**) Histogram of mean diameters (in cm) of *Gaojiashania* specimens (n = 30) and their frequency. **B**) BIC cluster analysis graph using mean diameters of *Gaojiashania* specimens (n = 30). Key: E = equal variance; V = unequal variance. Number of components indicates the possible number of populations inferred, based on mean diameter.

part of the Esmeralda Member (Corsetti and Hagadorn 2003), treptichnid-like trace fossils recording Cambrian-style, three-dimensional infaunal burrowing by Ediacaran meiofauna and small macrofauna are present
in underlying strata in both the lower Dunfee and lower Esmeralda members, including intervals hosting tubular macrofossils (Tarhan et al. 2020).

MATERIALS AND METHODS

The tubular fossils investigated in this study were collected from the Deep Spring Formation at Mount Dunfee (Fig. 1). Fossil samples were recovered principally from local float at localities E1515, E1425, and PLE2 (Fig. 2) and correlated to horizons in the lower Dunfee Member. In total, approximately 35 slabs containing *Gaojiashania* specimens were collected; a subset of 30 moldically preserved specimens, characterized by the highest-fidelity preservation, were analyzed in detail for this study. Specimens are reposited at the Smithsonian Institution National Museum of Natural History (USNM).

Gaojiashania specimens, including paired and unpaired casts and molds as well as composite molds (combined internal and external molds), preserved in siltstones and fine-grained sandstones, were photographed and examined under light microscopy (Fig. 3). The width of the transverse ring features (equivalent to the diameter of the compressed moldic fossil) and the preserved length of each tube were measured. A Shapiro-Wilk test was performed to test for normality of the diameter data and the skewness of the distribution was calculated. The programming software used for the statistical analyses was R Studio Version 2023.06.1 + 524 (2023.06.1 + 524). A Bayesian Information Criterion (BIC) cluster analysis was conducted through the R Studio `mclust` package to estimate the best model fit (the highest BIC value) for clusters in the dataset, based on mean diameter, assuming normality (Fig. 4; see Online Supplemental File) (Fraley and Raftery 2007; Hall et al. 2015). Morphometric data were used to confirm the diagnosis of these fossils as *Gaojiashania* (cf. Zhang et al. 1992; Cai et al. 2013). A literature compilation of morphological observations and measurements (Table 1) was used to compare and differentiate the Dunfee Member fossils from other reported specimens of *Gaojiashania* and other morphologically similar Ediacaran tubular fossils.

Thin sections (n = 8) were prepared to capture different orientations (both longitudinal and transverse) through *Gaojiashania* specimens and their relationship to associated strata (Online Supplemental File Fig. S1). These were examined via transmitted and polarized light microscopy, and petrographic features were photographed in transmitted and reflected light. All thin sections were examined using scanning electron microscopy (SEM) to characterize the fossils and associated sedimentary fabrics at higher resolution using a Hitachi SU7000 scanning electron microscope in the Earth Materials Characterization Center of the Department of Earth and Planetary Sciences at Yale University. The SEM was operated at an accelerating voltage of 15 kV and a working distance of 6 mm. Energy-dispersive spectroscopy (EDS) was used to generate elemental maps and facilitate mineral identification. SEM-EDS point-and-ID spectra and elemental weight percent (wt%) data (n = 35 spectra) were used to quantify elemental stoichiometries and identify minerals (see Online Supplemental File Tables S2, S3). Mineral composition was calculated for areas immediately adjacent to fossils and for the surrounding sedimentary matrix.

RESULTS

Morphometric Observations and Identification of Gaojiashania

The Dunfee specimens previously identified as *Gaojiashania* (Smith et al. 2016) are characterized by uniform width along an unbranched tube, and the tubes are comprised of rings of approximately equal thickness (Fig. 3A–3C). Folding and bending of the tube, as well as wrinkling of the rings, are present in four of the specimens, but deformation is limited and generally localized to the outer margins (Fig. 3E, 3G, 3H). Although specimens were likely taphonomically truncated in many instances, evidence for a holdfast or tapered terminal body is lacking. In several instances, fossils on bedding-plane surfaces are directly adjacent to subangular to subrounded granule- to pebble-sized mudstone intraclasts (Fig. 3D, 3F).

The fidelity of preservation of rings (Fig. 3) is greater in fine-grained, sandstone-dominated specimens compared to those in siltstone (Fig. 3A, 3G). The mean diameter of the rings is 5.76 mm (n = 81 measurements from 30 specimens; Fig. 4A) and the mean length of the Dunfee fossils is 32 mm (n = 30 measurements from 30 specimens). A Shapiro-Wilk test ($p = 0.00879$, where $\alpha = 0.05$) indicates that a normal distribution can be rejected for these diameter data and that the distribution represents a

TABLE 1.—*Literature compilation of geographic, stratigraphic, morphological and taphonomic data for Ediacaran tubular fossils broadly comparable to the Dunfee Member* Gaojiashania *assemblage described in this study.*

Fossil	Region	Stratigraphic occurrence	Age	Fossil diameter	Fossil length	Interpretation	Preservational mode(s)	Reference
Gaojiashania	Shaanxi Province, South China	Gaojiashan Lagerstätte, Dengying Fm	Upper Ediacaran	>10 mm	N/A	Body fossil	Pyritization, glauconite replacement, kerogenization	Cai et al. 2010
Gaojiashania annulcosta	Siberian Platform	Yudoma Group	Upper Ediacaran	1–4 mm	<100 mm	Body fossil	Silicification	Zhuravlev et al. 2009
Gaojiashania caperata	South China	Gaojiashan Lagerstätte, Dengying Fm	Upper Ediacaran	7–8 mm	~50 mm	Body fossil	Calcification	Cai et al. 2013
Gaojiashania cyclus	South China	Gaojiashan Lagerstätte, Dengying Fm	Upper Ediacaran	7–9 mm	50–60 mm	Body fossil	Pyritization, aluminosilicification, kerogenization	Cai et al. 2013
Gaojiashania haihaoliangensis	South China	Gaojiashan Lagerstätte, Dengying Fm	Upper Ediacaran	1.25 mm	1.5 mm	Body fossil	Calcification	Cai et al. 2013
Gaojiashania zonatas	South China	Gaojiashan Lagerstätte, Dengying Fm	Upper Ediacaran	7–9 mm	90–120 mm	Body fossil	Pyritization	Cai et al. 2013
Gaojiashania	Nevada, USA	Deep Spring Fm, Dunfee Member	Upper Ediacaran	3–13 mm	15–100 mm	Body fossil	Ediacara-style (casts and molds)	Smith et al. 2016; this study
Gaojiashania	Nevada, USA	Wood Canyon Fm., Nevada	Upper Ediacaran	0.2–10 mm	27–65 mm	Body fossil	Pyritization	Smith et al. 2017
Gaojiashania annulcosta	South China	Gaojiashan Lagerstätte, Dengying Fm	Upper Ediacaran	8–12 mm	45–62 mm	Body fossil	Calcification	Cai et al. 2013
Shaanxilithes ningqiangensis	Shaanxi Province, South China	Gaojiashan Lagerstätte, Dengying Fm	Upper Ediacaran	1–6 mm	N/A	Body fossil	Kerogenization	Cai et al. 2010
Shaanxilithes	North China Craton and Qaidam Block, North China	Tuerkeng Fm and Zhoujieshan Fm	Upper Ediacaran	0.3–5.1 mm and 0.8–11mm	<180 mm	Body fossil	Kerogenization	Wang et al. 2021
Shaanxilithes ningqiangensis	Shaanxi Province, South China	Gaojiashan Member, Dengying Fm	Ediacaran	5–8 mm	5–10 cm	Trace fossil	Aluminosilicification	Weber et al. 2007
Shaanxilithes ningqiangensis	South China	Dengying Fm	Ediacaran	0.8–9.5 mm	N/A	Trace fossil	N/A	Hua et al. 2000
Shaanxilithes ningqiangensis	South China	Dengying Fm	Ediacaran	0.8–9.5 mm	N/A	Body fossil	N/A	Hua et al. 2004
Shaanxilithes ningqiangensis	South China	Dengying Fm	Ediacaran	>5 mm	N/A	N/A	N/A	Shen et al. 2007
Shaanxilithes ningqiangensis	Siberian Platform	Yudoma Group	Upper Ediacaran	1–4 mm	<100 mm	N/A	Silicification	Cai et al. 2011a
Shaanxilithes ningqiangensis	Shaanxi Province, South China	Dengying Fm	Upper Ediacaran	0.8–7.8 mm	9.9–95.0 mm	Body fossil	Aluminosilicification	Meyer et al. 2012
Shaanxilithes ningqiangensis	Lesser Himalaya, India	Krol Group and Tal Group	Upper Ediacaran (–lower Cambrian?)	0.33–14.63 mm	1.19–54.67 mm	Body fossil	Kerogenization and phosphatization	Tarhan et al. 2014
Shaanxilithes ningqiangensis	Yangtze Gorge Area, South China	Dengying Fm	Upper Ediacaran	N/A	<85 mm	N/A	N/A	An et al. 2020
Shaanxilithes ningqiangensis	Huize, Yunnan Province, China	Dengying Fm	Upper Ediacaran	2–20 mm	N/A	N/A	N/A	Fang et al. 2022
Shaanxilithes ningqiangensis	North China Craton and Qaidam Block, North China	Tuerkeng Fm and Zhoujieshan Fm	Upper Ediacaran	1.3–4.1 mm and 0.8–9.5 mm	<180 mm	Body fossil	N/A	Wang et al. 2021
Shaanxilithes ningqiangensis	Shaanxi Province, South China	Doushantou Fm and Dengying Fm	Uppermost Ediacaran	0.3–8 mm	50–80 mm	Body fossil	Kerogenization	Chai et al. 2021
Sinotubulites baimatuoensis	Shaanxi Province, South China	Gaojiashan Lagerstätte, Dengying Fm	Upper Ediacaran	1.5–6 mm	3–28 mm	Body fossil	Calcification, phosphatization, dolomitization	Cai et al. 2015

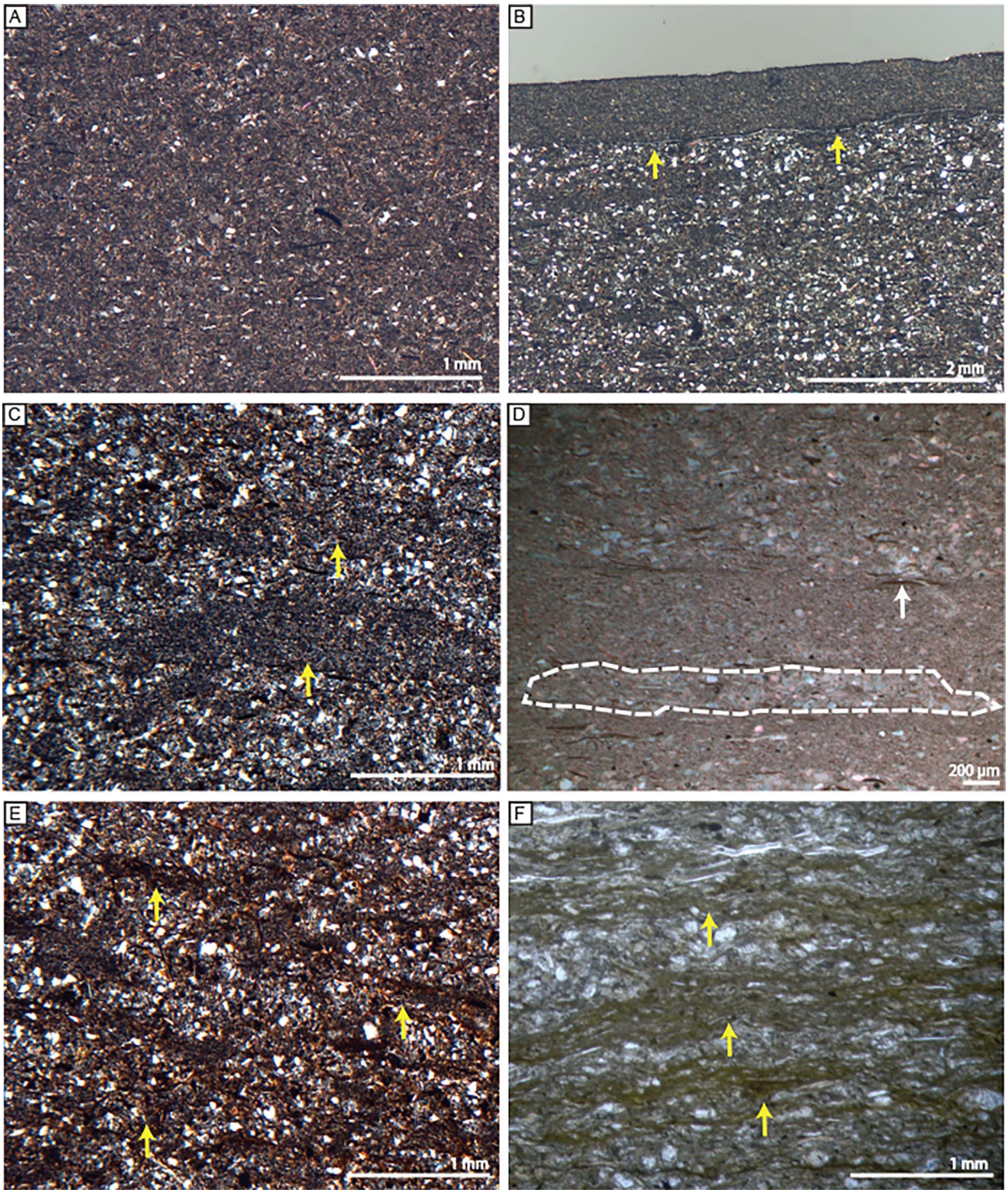

FIG. 5.—Petrographic thin-section photomicrographs illustrating different textural and mineralogical characteristics of *Gaojiashania*-bearing samples. **A**) Composition of siltstone sample USNM-PAL-794720 in plane-polarized light (PPL). **B**) Spatial relationship of fossil-bearing area (upper portion, in this orientation) to surrounding sediments (lower portion) of sample USNM-PAL-794719 illustrating the finer-grained texture of the fossil area compared to surrounding sediments with coarser average grain size, as viewed in PPL (yellow arrows denote boundary between these two textural zones). However, mineral composition is similar between these two texturally disparate zones. **C**) Areas of finer-grained material (indicated by yellow arrows) in the matrix of sample USNM-PAL-794719 indicate potential intrastratal fossiliferous regions or mudstone intraclasts; PPL. **D**) Quartz aggregates indicated by the white dashed-line region; dark, elongate minerals indicated by the white arrow (e.g., USNM-PAL-794709). **E**, **F**) Crinkly laminated fabric, interpreted as possible textural remnants of microbial mats, subsequently replaced by clay minerals, denoted by yellow arrows in sample USNM-PAL-794709 (E) and USNM-PAL-794718 (F); PPL.

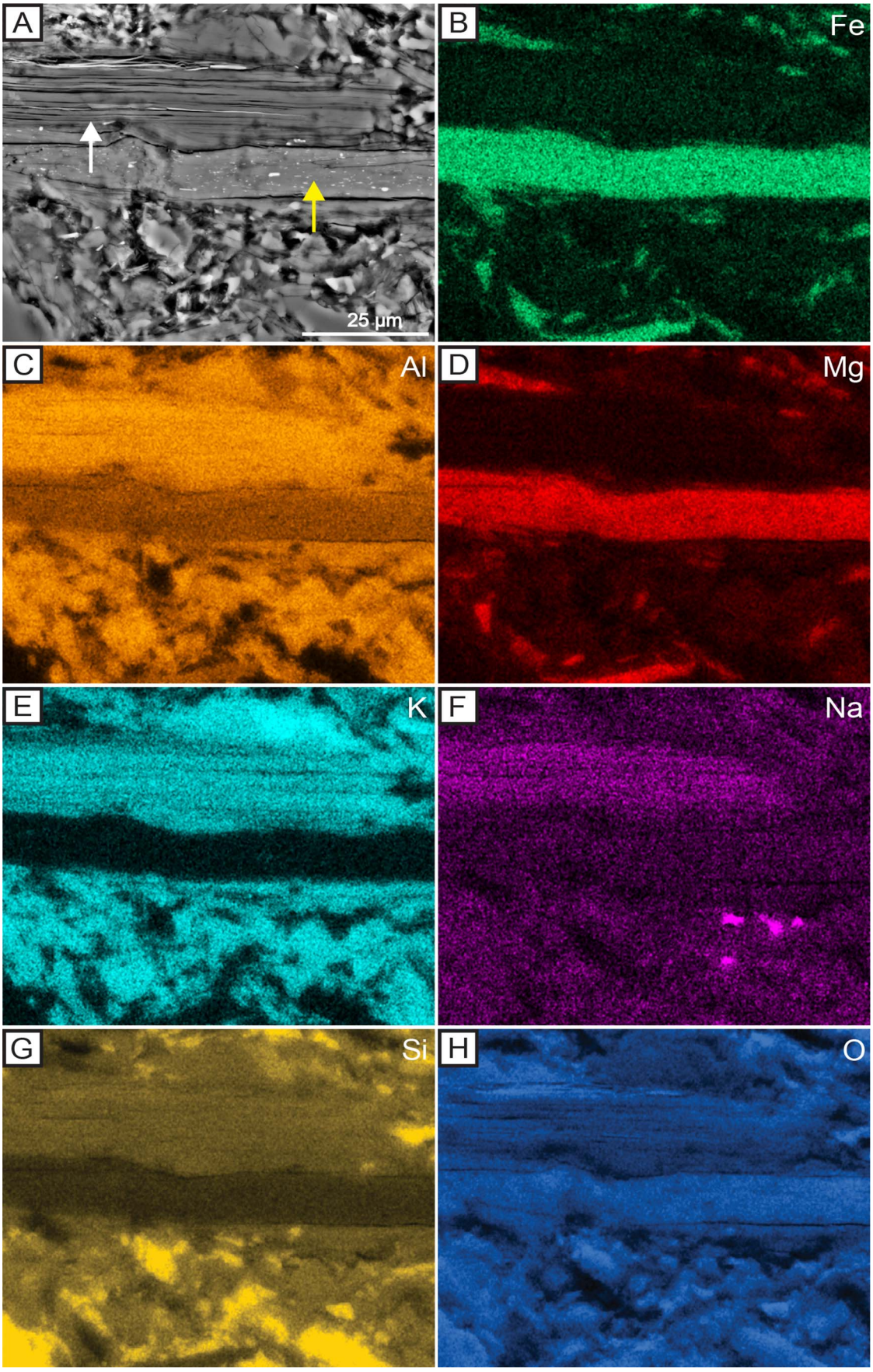

skewness of +0.773, reflecting a right-skewed distribution. A BIC cluster analysis was applied to the mean diameter of individual specimens, yielding nine different models describing equal-variance (E) clusters and seven unequal-variance (V) clusters of different sizes. The best-fit models were (E, 3), (E, 2), and (V, 2), with BIC values of -11.4, -11.7 and -11.7, respectively. Higher BIC values reflect a better model fit (Fig. 4B). Our cluster analysis, albeit based on a small number of samples, may suggest either that the Dunfee *Gaojiashania* assemblage represents multiple populations or that it is parautochtonous (see below).

The Dunfee fossils differ from annulated cloudinomorphs in the absence of tapering of the tubes (Cai et al. 2014, 2017; Yang et al. 2022). The 25th and 75th percentiles of the Dunfee the Dunfee fossil diameters are 5.25 mm and 10.2 mm, respectively, and the Dunfee specimens are similar in length to those of *Gaojiashania cyclus* from the Gaojiashan Lagerstätte (Table 1), which range from 5 to 60 mm in length and 7 to 9 mm in diameter (Cai et al. 2013). The annulated tubular fossil *Shaanxilithes* is 1.19–54.67 mm in length and 0.50–13.53 mm in diameter in assemblages from the Ediacaran–Cambrian transition of the Krol and Tal groups of India (Tarhan et al. 2014), where it is preserved as carbonaceous and partially phosphatized compressions. Additionally, while distances between annulations are uniform in *Gaojiashania*, *Shaanxilithes* has been inferred to be composed of crescent rings, separated by uneven distances, that resemble funnel-in-funnel structures similar to *Cloudina* (Wang et al. 2021). *Shaanxilithes* is also commonly characterized by a unique 'ribbon-like' texture resembling tightly curved and/or overlapping ribbons (e.g., Meyer et al. 2012)—a morphology not documented for *Gaojiashania* and which we do not observe in the Dunfee assemblage. In light of these observations, although the size range of the Dunfee Member *Gaojiashania* overlaps with the reported size range of both *Gaojiashania* and *Shaanxilithes* in other deposits, these two taxa characteristically differ in size distribution, morphology, and preservational style. We therefore assign the Dunfee Member specimens to *Gaojiashania*, based on similarity in size range and the presence of readily identifiable rings consistent with material previously described from South China and elsewhere (Table 1).

Petrographic Observations of Gaojiashania *Taphonomy*

Petrographic analyses indicate that the fine-grained sandstone and siltstone strata hosting the Dunfee *Gaojiashania* are texturally and compositionally immature, consisting predominantly of quartz and phyllosilicates, as well as opaque minerals (Fig. 5). There is a notable disparity in grain size between the areas immediately adjacent to some of the fossils (finer-grained) and surrounding sediments (coarser-grained) (Fig. 5B). Ovoid to elongate mudstone intraclasts ($\sim$ 500 μm in width and $\sim$ 0.9–4 mm in length) are abundant along hand-sample bedding planes, and thin sections reveal that they are also present intrastratally (Fig. 5C, 5D). In some instances, thin layers of quartz-rich aggregates are associated with these finer-grained, potentially fossiliferous, and/or intraclastic intrastratal regions (Fig. 5D).

Sheet-like phyllosilicate minerals are common in *Gaojiashania* samples. Pyrite framboids and euhedra, as well as framboidal pyrite pseudomorphs, are rare. Oxides were identified via optical microscopy by their euhedral, opaque, and pleochroic nature (Fig. 5E). Other opaque, crystalline, and arcuate grains are also present (Fig. 5A, 5C, 5D). These minerals are not typically uniformly oriented parallel to bedding except where they make up larger aggregates (Fig. 5C, 5D). Optically dark, small (0.5–1 mm), elongate aggregates showing arcuate textures and longer ($\sim$ 6 mm) crinkly (i.e., wavy) structures, oriented parallel to bedding (Fig. 5E, 5F), are more common in siltstone samples (e.g., samples USNM PAL 794709 and USNM PAL 794722). These crinkly aggregates (Fig. 5F) are texturally reminiscent of organic filaments associated with *Gaojiashania* in the Gaojiashan Lagerstätte, which have been interpreted as remnants of microbial mats (Cai et al. 2010, 2014). The mudstone intraclasts of the Dunfee samples (see above) differ from the opaque aggregates in their lack of a crinkly morphology, large diameter, and variable length (Fig. 5C).

SEM and EDS Observations and Mineralogical Composition of Gaojiashania *Samples*

SEM and EDS analyses of *Gaojiashania* samples in thin section provided higher-resolution data of the compositional and textural features of *Gaojiashania* and hosting sediments (Figs. 6–8). SEM imaging corroborates the difference in grain size between the moldically preserved fossils and surrounding sediments. However, this difference is principally textural rather than compositional; the finer-grained matrix surrounding *Gaojiashania* molds is similar in composition to coarser-grained matrix further from the fossil. Mineralogical results described below therefore include both fossil-proximal and fossil-distal regions of thin sections unless stated otherwise (Online Supplemental File Fig. S1).

Gaojiashania-hosting beds contain abundant silt- and sand-sized grains of detrital quartz, less abundant orthoclase and plagioclase feldspar, and rare apatite (Figs. 6–8). Both the finer-grained areas surrounding *Gaojiashania* fossils, and the adjacent siltstone and very fine-grained sandstone matrix, are dominated by aluminosilicates associated with enrichments of Al, K, and Si (Figs. 6–8). Mg- and Fe-rich clays, both aluminous and non-aluminous (Fig. 6), are also present. We interpret these phyllosilicates as a combination of detrital and authigenic clays, the latter potentially representing multiple generations of authigenesis. Mg- and Fe-rich clays, for example, commonly surround and are attached to K-rich aluminous clays (Fig. 7). Rare iron oxides are not spatially associated with the fossils; they are not framboidal, mostly infill late-forming fractures, and are associated with weathering rinds (Online Supplemental File Fig. S2). Local enrichments of Na and O in conjunction with elevated Si may indicate the presence of additional clay minerals such as zeolites.

Fe- and Mg-rich non-aluminous clays are commonly aligned parallel to bedding. They are typically compactionally deformed in the immediate vicinity of both aluminosilicates and detrital feldspar, quartz, and apatite grains (Figs. 7, 8). Other Fe- and Al-rich clays are randomly oriented relative to bedding and are not aligned with other grains, suggesting an authigenic origin (Fig. 8). Some of these minerals exhibit 'booklet' textures characteristic of a range of clay mineral groups, such as kaolinite and chlorites (Figs. 6–8). Some Al- and Fe-rich minerals are rimmed by additional Al-rich clay minerals, which may reflect different episodes of nucleation-mediated authigenesis or the presence of both detrital (in this case, Fe-rich) and authigenic aluminosilicates (Figs. 6, 7). Fe- and Mg-rich clay minerals in the pore spaces between detrital mineral grains may indicate authigenic porosity infill. Authigenic clays also infill more porous (e.g., partially dissolved or exsolved) Fe-rich minerals. SEM-

←

FIG. 6.—SEM-EDS elemental maps for sample USNM-PAL-794719. **A)** SEM back-scatter image of a juxtaposed aluminosilicate (white arrow) and a relatively aluminum-poor, Fe- and Mg-rich clay mineral (yellow arrow) surrounded by a matrix of finer-grained aluminous and K- and Na-rich minerals and quartz. **B–H**) Fe (B) and Mg (D) are concentrated in the clay mineral in the center of the frame (denoted by the yellow arrow in panel A), with lower abundances of Al (C) and Si (G). This Fe- and Mg-rich clay is in turn surrounded by clays more strongly enriched in Al (C), K (E) and Na (F) (denoted by white arrow). Distribution of O also shown in (H). Scale bar in (A) pertains to all panels. See Online Supplemental File Fig. S1 for additional information regarding location of mapped area.

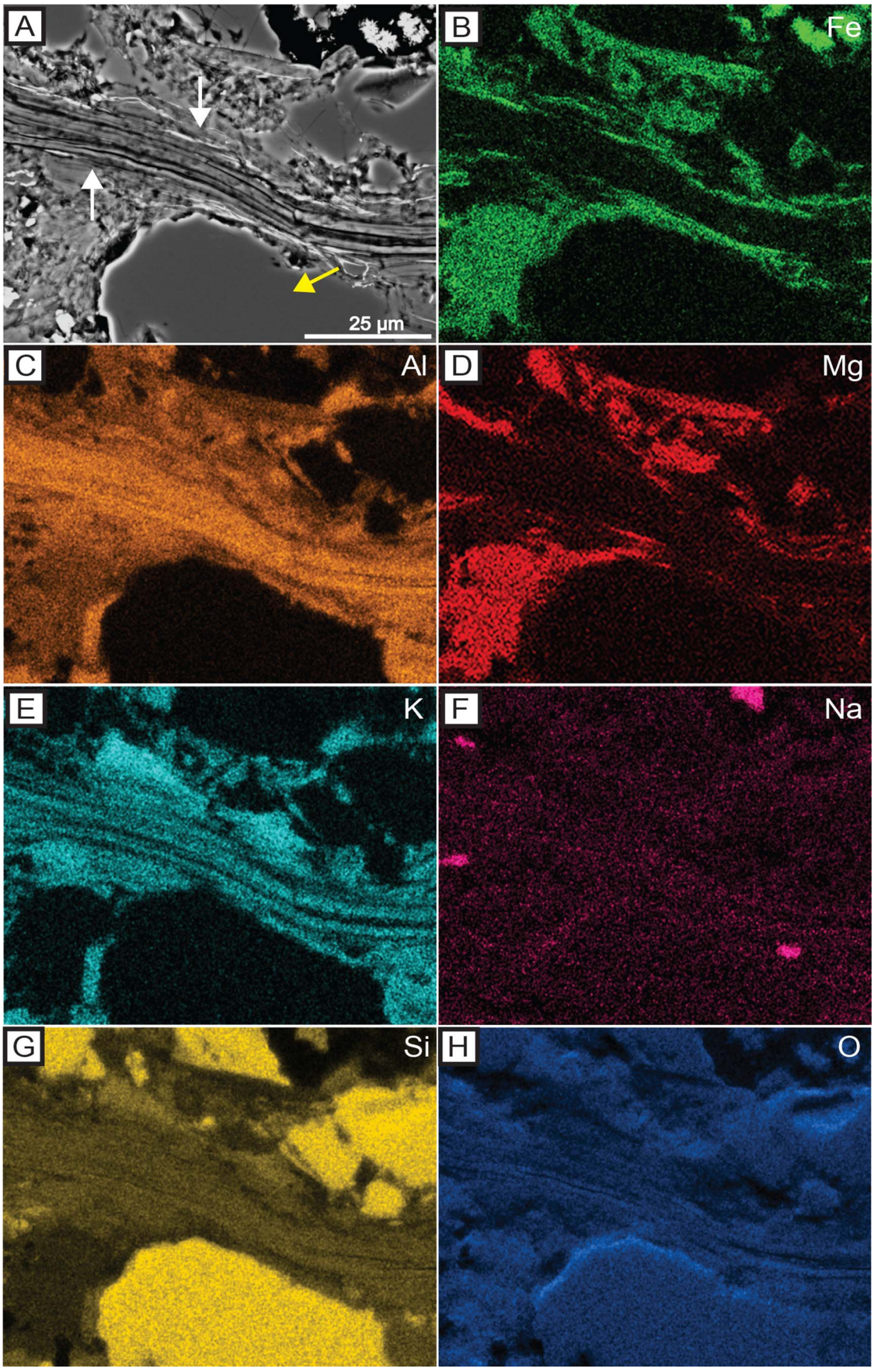

EDS observations indicate that the crinkly laminae that were observed petrographically (Fig. 5E, 5F) consist of bedding-parallel assemblages of Mg- and Fe-rich clay minerals.

Stoichiometric identification of mineral compositions from EDS spectral data (Online Supplemental File Fig. S3–S37) confirms the presence of a variety of clay minerals, in addition to abundant quartz and less abundant feldspars and apatite (Online Supplemental File Table S3). Phyllosilicates include, but are not limited to, the clay minerals chamosite, glauconite, clinochlore, and odinite, in addition to micas such as lepidolite, muscovite, and biotite. This assemblage includes authigenic clay minerals such as glauconite, as well as metamorphic-grade minerals, such as clinochlore and muscovite, that may have been derived from either authigenic clay or detrital precursors. The presence of chamosite, a common product of the alteration or thermal maturation of berthierine, may also indicate an authigenic precursor phase (Bailey 1988; Hornibrook 1996). Authigenic minerals surrounding feldspar and other detrital grains are chlorite or, in some cases, unidentified Fe-rich phyllosilicates. Thirty spectra were identified using this approach (Online Supplemental File Fig. S3–S39, Tables S2, S3). An additional five spectra, containing Al, Fe, and Mg, could not be readily stoichiometrically assigned to specific clay mineral groups, although both molar abundances and textures indicate a phyllosilicate affinity. Thus, they are placed in a general "phyllosilicate" category (Online Supplemental File Fig. S33–S37, Table S3). Spectral EDS analyses indicate that clay minerals, including non-aluminous Fe- and Mg-rich minerals, are abundant in all thin sections (Figs. 6–8).

DISCUSSION

A Body Fossil Affinity for the Dunfee Gaojiashania

The affinity of *Gaojiashania*—specifically, whether it is a body or trace fossil—has been debated (Zhuravlev et al. 2009; Cai et al. 2011a) but our biostratinomic observations support a body fossil interpretation for the Dunfee fossils. Gentle curves may be characteristic of trace fossils, but the high-angle bending, overfolding (i.e., overlapping rather than cross-cutting relationships), and plastic deformation recorded in multiple Dunfee Member specimens are inconsistent with a trace fossil affinity (cf. Jensen 2003; Jensen et al. 2006). Bending and folding of individual specimens may reflect deformation during transport and/or burial of the carcass. The lack of evidence for a holdfast may also support previous inferences (Cai et al. 2013) that *Gaojiashania* lived prone on the seafloor. The lack of complete specimens and commonly irregular terminations of the Dunfee specimens suggest that they may represent a parautochthonous or allochthonous assemblage; close association with bedding-plane accumulations of subangular to rounded mudstone intraclasts is further evidence for transport. However, the high fidelity of preservation of these specimens, lack of disarticulation (in contrast to transported *Gaojiashania* in the Gaojiashan Lagerstätte) (Cai et al. 2010), lack of alignment, and the poorly sorted nature of both intraclasts and fossils suggest that their transport was limited.

Association of Gaojiashania *with Iron-Rich Clay Minerals*

Previous studies have suggested that Fe-rich minerals associated with assemblages of *Gaojiashania* in South China and the Death Valley region of the western USA may represent pyrite (or its oxidized remnants), as evidenced by the presence of Fe- and S-rich framboids associated with South China specimens (Cai et al. 2010, 2012) and macroscopic iron oxide coatings associated with Death Valley specimens (Smith et al. 2017, 2023). However, SEM-EDS observations of Fe-rich phases associated with the Dunfee *Gaojiashania* indicate that they are similarly enriched in Mg and Si, and are not framboidal, but instead are characterized by tabular to sheet-like phyllosilicate morphologies (Figs. 6–8). We therefore diagnose these minerals as Fe- and Mg-rich clays. Some of the Fe-enriched aluminous clays include glauconite. Iron oxides are rare and represent late-stage textures, e.g., late-stage fracture infill (Online Supplemental File Fig. S2) and weathering rinds. Therefore, neither oxides nor pyrite appear to have influenced the fossilization of the Dunfee *Gaojiashania*. The Fe-rich minerals in *Gaojiashania*-hosting strata of the Dunfee Member are primarily authigenic clay minerals that we interpret to have formed through precipitation on detrital clays and other detrital grains as well as associated organic matter during early diagenesis (Fig. 9).

A Taphonomic Role for Clay Minerals

Our investigation indicates that the Dunfee Member *Gaojiashania* are characterized by a distinct mode of moldic, Ediacara-style preservation that was strongly shaped by clay authigenesis. The clay-rich mineralogy and moldic preservation of *Gaojiashania* are distinct from the preservation of other tubular fossils previously characterized from this locality, including calcified cloudinomorphs in the Dunfee Member and pyritized *Costatubus bibendi* and *Saarina hagadorni*, previously assigned to *Conotubus*, in the Esmeralda Member (Smith et al. 2016, 2023; Selly et al. 2020). Textural and mineralogical observations indicate that much of the clay in the Dunfee Member *Gaojiashania* specimens is authigenic in origin and that authigenic clay minerals may have played a key role in their fossilization. At the thin-section scale, the relative abundance of clay-sized particles (both detrital and authigenic) in the matrix is greater in the immediate vicinity of *Gaojiashania* specimens, suggesting that some of the textural difference between fossil-proximal and fossil-distal regions may reflect synsedimentary differences in deposition. However, there are no consistent differences in the mineralogy of the matrix immediately proximal and more distal to the fossils. Both detrital and authigenic clay minerals occur in each region indicating that early diagenetic transformation of sediments templating *Gaojiashania* must have likewise impacted the surrounding sediment. Accumulation of transported fragments of microbial mats (Fig. 5F) or other detrital, fine-grained organic matter at various horizons in these strata may have promoted early diagenetic clay mineral authigenesis and replacement of these fine-grained organic fragments by means of sedimentary microbial iron reduction.

Gaojiashania occurs in a variety of preservational modes globally, including assemblages in Siberia (Zhuravlev et al. 2009), South China

←

FIG. 7.—SEM-EDS elemental maps for sample USNM-PAL-794709. SEM back-scatter image of elongate booklet of aluminous clay (white arrows) surrounded by a Fe-, Mg-, and K-enriched matrix. EDS data indicate that the clay booklet in the center of the frame is enriched in Al (C) and K (E), with lower relative abundances of Si (G) and O (H) and trace amounts of Na (F). In contrast, surrounding finer-grained clay matrix is enriched in Fe (B), Al (C), Mg (D) and K (E), as well as Si (G) and O (H). Particularly pronounced Si (G) enrichments are associated with detrital quartz grains (e.g., yellow arrow in panel A). Sparse finer-grained detrital albite grains are characterized by Na (F), Al (C), Si (G) and O (H) enrichments. Scale bar in (A) pertains to all panels. See Online Supplemental File Fig. S1 for additional information regarding location of mapped area.

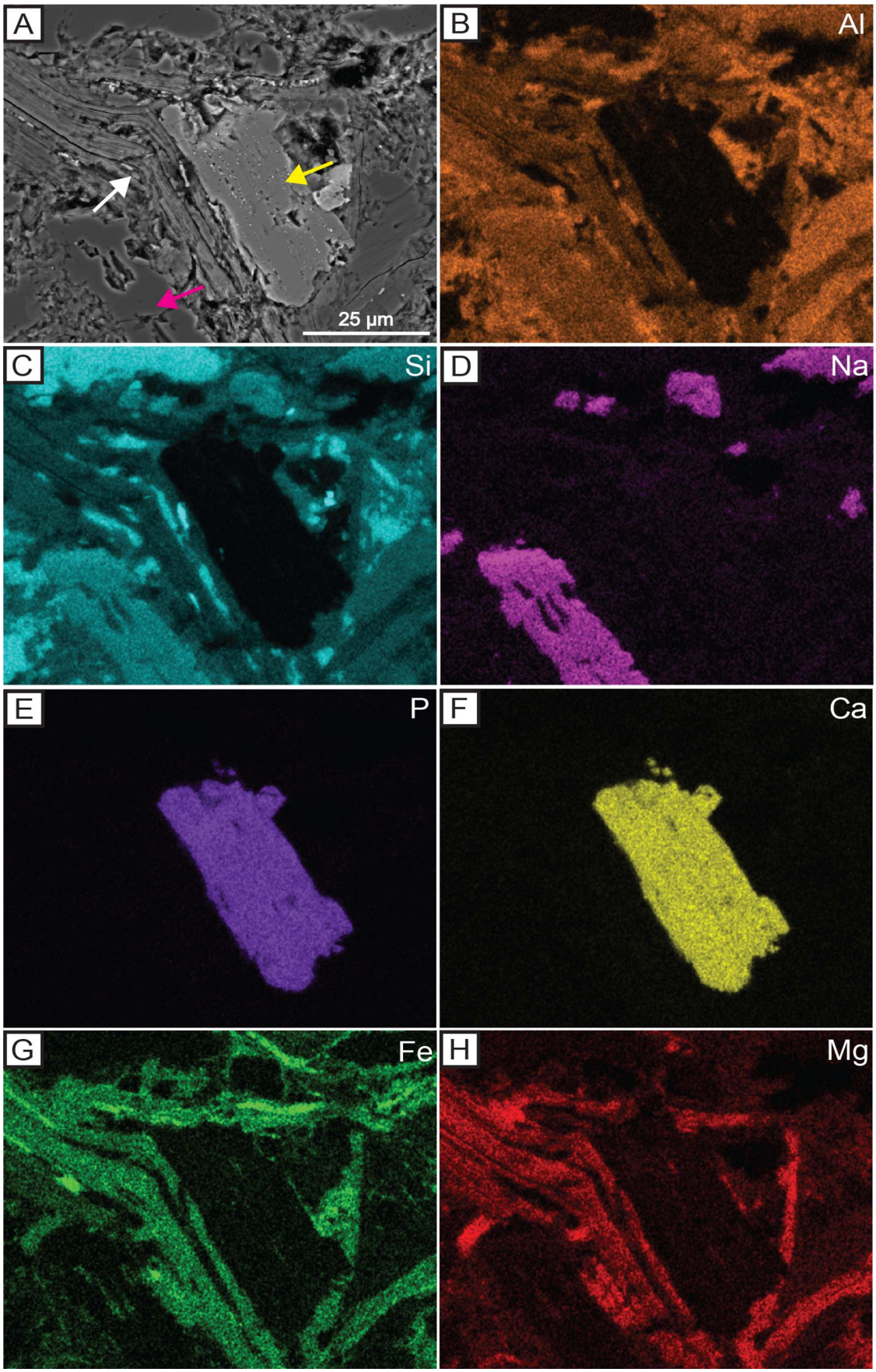

(Cai et al. 2010, 2012; Chen et al. 2022), Namibia (Smith et al. 2017), and the Death Valley region of Nevada (Smith et al. 2017, 2023). Pyritization is one of the most common taphonomic modes of *Gaojiashania* assemblages (Cai et al. 2010, 2012; Smith et al. 2017). However, *Gaojiashania* specimens replaced by glauconite have also been documented in the Gaojiashan Member in South China (Cai et al. 2010, 2013). The Dunfee *Gaojiashania* assemblage, in contrast, is not replaced by clay but is moldically preserved in a sedimentary matrix rich in aluminous and non-aluminous Fe- and Mg-rich clays. The presence of finely disseminated reactive organic matter, in the form of microbial rip-up fragments, coupled with the large size of *Gaojiashania* carcasses, may have prevented clay replacement of the latter (analogous to the impact of disseminated organic matter on macrofossil pyritization; cf. Raiswell et al. 1993) and instead promoted moldic preservation of *Gaojiashania* by authigenic clay-enriched surrounding sediments.

Iron-rich authigenic clay minerals may form either through transformation of detrital phases or via porewater precipitation from dissolved ferrous iron (Deocampo 2015; Isson and Planavsky 2018; Han et al. 2022, 2024). Iron cycling, including ready availability of highly reactive ferric iron substrates for microbial iron reduction and porewater accumulation of ferrous iron, may in turn have been fostered by the ferruginous seawater conditions reconstructed for many Ediacaran marine settings (Sperling et al. 2015). Local sedimentary iron reduction, fueled by higher global and local availability of highly reactive iron phases, as well as the availability of detrital clay minerals as nucleation sites for authigenic clay phases, may likewise have played a critical role in the formation of iron-rich clay minerals associated with the Dunfee Member *Gaojiashania*.

Ediacaran seawater was substantially enriched in dissolved silica relative to the modern oceans, prior to the radiation of silica-biomineralizing organisms such as sponges, radiolarians, and diatoms (Maliva et al. 1989; Siever 1992). These high seawater silica levels have been proposed to have enhanced the rate and extent of silica authigenesis (e.g., Maliva et al. 1989), including facilitating multiple modes of exceptional fossilization—such as Ediacara-style moldic preservation of soft-bodied macrofossils via early silica cementation of sandy sediments (Tarhan et al. 2016; Slagter et al. 2024b) and Bitter Springs-style permineralization of organic-walled microfossils in cherts (e.g., Butterfield 2003). Compilations of mineral assemblage data, modeling-based studies, and experiments have also suggested that high dissolved silica levels in Precambrian oceans may have fostered extensive authigenic clay formation or reverse weathering (Isson and Planavsky 2018; Trower and Fischer 2019), a factor that was potentially important in Dunfee Member sediments (Fig. 9) as well as other Ediacara-style fossil deposits (Slagter et al. 2024a). Hydrothermal vent systems can, in the modern ocean, supply high concentrations of dissolved silica and promote local precipitation of authigenic siliceous phases, including clay minerals (e.g., Grasse et al. 2020). However, hydrothermal dissolved silica enrichments are rapidly diluted by surrounding seawater (e.g., Brzezinski and Jones 2015; Geilert et al. 2020; Grasse et al. 2020; Fitzsimmons and Steffens 2024). There is no direct evidence for syndepositional hydrothermal activity in the Dunfee Member. Although the presence of potential syn-rift volcanics and volcaniclastic strata in Ediacaran and Cambrian strata elsewhere in the Great Basin (e.g., Smith et al. 2023) may indicate a hydrothermal influence in this region, any hydrothermal contributions of dissolved silica to the seafloor settings recorded by the Dunfee Member would likely have been negligible relative to elevated background seawater levels.

Extensive reverse weathering during the Proterozoic and Cambrian may have contributed to multiple modes of fossilization linked to authigenic clay enrichments, including replacement of both soft-bodied and shelly fossils by clay minerals (e.g., Cai et al. 2013; Pruss et al. 2019), Burgess Shale-type preservation of carbonaceous compressions (e.g., Anderson et al. 2018) and Ediacara-style moldic preservation (e.g., Laflamme et al. 2011; Hall et al. 2020; Slagter et al. 2024a; this study). The high abundance of authigenic clay minerals associated with the Dunfee Member *Gaojiashania* specimens reflects the importance of clay authigenesis in facilitating the moldic preservation of late Ediacaran macrofossils in heterolithic and compositionally immature siliciclastic lithofacies. This taphonomic pathway may have shaped exceptionally preserved fossil deposits ranging from Neoproterozoic to lower Paleozoic in age, i.e., the interval characterized by the intersection of (1) benthic populations of (more readily fossilized and identified) morphologically complex macroorganisms and (2) globally silica-enriched and locally ferruginous ocean waters. These data highlight the need for a more detailed consideration of moldic fossilization in heterolithic and compositionally immature facies, as well as a more mechanistic exploration of the factors favoring clay precipitation relative to other modes of silica or iron authigenesis.

CONCLUSIONS

The high abundance of Mg- and Fe-rich clay minerals in *Gaojiashania*-bearing strata of the Dunfee Member of the Deep Spring Formation indicates that authigenic clays played a significant role in the preservation of these fossils. These data illustrate that authigenic clay minerals, particularly in heterolithic and compositionally immature lithofacies like those of the Dunfee Member, may have directly facilitated the moldic preservation of upper Ediacaran tubular fossils like *Gaojiashania* by cementing surrounding detrital grains and forming molds that templated the morphology of these organisms. The mechanisms by which these (and other) tubular organisms were fossilized may have strongly shaped the stratigraphic distribution of candidate upper Ediacaran index fossils like *Gaojiashania* and thus interpretations of the timing and pace of the rise of animals. Additionally, the mineralogical and petrographic data provided by the Dunfee Member specimens indicate that authigenic clay-mediated moldic fossilization of unmineralized taxa such as *Gaojiashania* may be linked to the prevalence of silica-rich and ferruginous seawater conditions prior to the radiation of silica-biomineralizing organisms or the final rise of ocean and atmospheric oxygen to modern levels.

ACKNOWLEDGMENTS

This research was supported by the NASA Exobiology Program (grant NNX14AJ86G to L.G.T and P.M.M. and grant 80NSSC19K0472 to L.G.T.), a NSF Earth Sciences Postdoctoral Fellowship (to L.G.T.), a Smithsonian Institution Peter Buck Postdoctoral Fellowship (to E.F.S.), the American Philosophical Society Lewis and Clark Fund for Exploration and Field

←

FIG. 8.—SEM-EDS elemental maps for sample USNM-PAL-794718. **A)** SEM-EDS back-scatter image of apatite (yellow arrow) and albite (pink arrow) grains surrounded by a clay matrix (e.g., white arrow). Deformation of the clay (white arrow) is inferred to be compactional, corroborating a detrital or early authigenic origin. Detrital apatite grain (yellow arrow) is characterized by enrichments in P (E) and Ca (F); detrital albite grains (e.g., pink arrow) are enriched in Na (D), Al (B), and Si (C). Surrounding coarser- and finer-grained clay matrix is variably enriched in Al (B), Si (C), Fe (G) and Mg (H). Scale bar in (A) pertains to all panels. See Online Supplemental File Fig. S1 for additional information regarding location of mapped area.

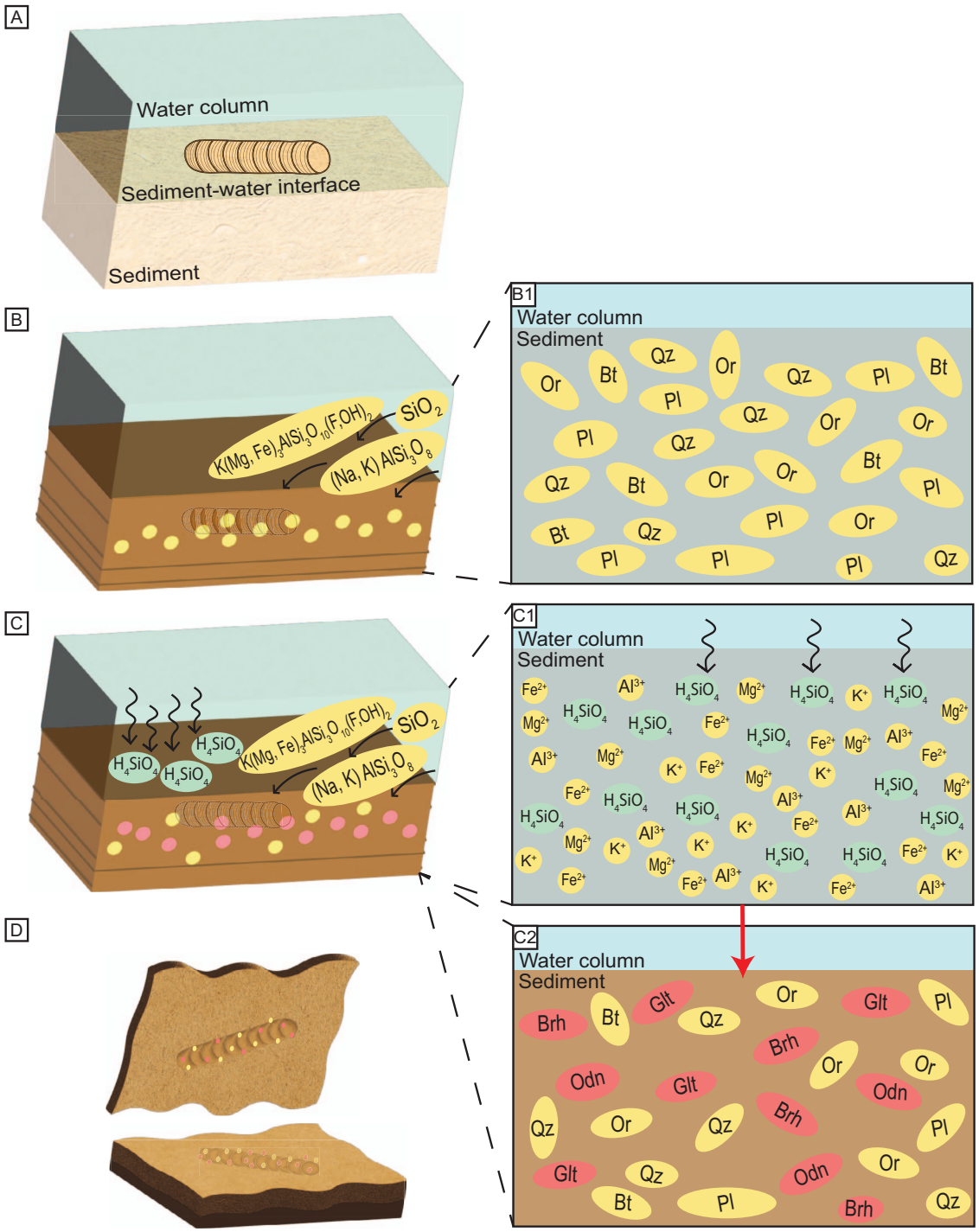

FIG. 9.—Schematic depicting reconstructed pathways of sedimentary diagenesis and fossilization of the Dunfee *Gaojiashania*. **A**) Living *Gaojiashania* lying prone on the seafloor. **B**, **B1**) The transport of detrital material (indicated by yellow circles and ellipses) associated with the burial of *Gaojiashania*. **C**) Authigenesis of *Gaojiashania* and surrounding sediments. **C1**) Cations liberated by porewater iron reduction and release of Mg, K, and Al from detrital mineral dissolution (yellow circles) combine with seawater-derived silicic acid (indicated by green ellipses) to precipitate authigenic clay minerals (indicated by red circles and ellipses in C). **C2**) The resulting sedimentary matrix contains both authigenic clays (red ellipses) and detrital minerals (yellow ellipses) that surround the fossil carcass during burial. **D**) *Gaojiashania*, preserved as part-counterpart cast and mold. Key: Bt = biotite; Pl = plagioclase; Or = orthoclase; Qz = quartz; Odn = odinite; Brh = berthierine; Glt = glauconite.

Research in Astrobiology (to E.F.S.), and the Palaeontological Association (grant PA-RG201703 to E.F.S.). We thank S. Butts, J. Ague, and Z. Jiang for assistance with sample imaging and SEM-EDS analyses, respectively; N. Planavsky for discussion; and J. Schiffbauer, S. Pruss and two anonymous reviewers for comments that improved this manuscript.

SUPPLEMENTAL MATERIAL

Data are available from the PALAIOS Data Archive: https://www.sepm.org/supplemental-materials.

REFERENCES

Amthor, J.E., Grotzinger, J.P., Schröder, S., Bowring, S.A., Ramezani, J., Martin, M.W., and Matter, A., 2003, Extinction of *Cloudina* and *Namacalathus* at the Precambrian–Cambrian boundary in Oman: Geology, v. 31, p. 431–434, doi: 10.1130/0091-7613(2003)031<0431:EOCANA>2.0.CO;2.

An, Z., Zhao, X., Niu, Z., Li, Z., and Ye, Q., 2020, Discovery of *Shaanxilithes* from the Dengying Formation in the Yangtze Gorges area, South China, and its stratigraphic significance: China Geology, v. 3, p. 649–651, doi: 10.31035/cg2020059.

Anderson, R.P., Tosca, N.J., Gaines, R.R., Mongiardino Koch, N., and Briggs, D.E.G., 2018, A mineralogical signature for Burgess Shale-type fossilization: Geology, v. 46, p. 347–350, doi: 10.1130/G39941.1.

Bailey, S.W., 1988, Odinite, a new dioctahedral-trioctahedral Fe 3+ -rich 1:1 clay mineral: Clay Minerals, v. 23, p. 237–247, doi: 10.1180/claymin.1988.023.3.01.

Bowring, S.A., Grotzinger, J.P., Isachsen, C.E., Knoll, A.H., Pelechaty, S.M., and Kolosov, P., 1993, Calibrating rates of early Cambrian evolution: Science, v. 261, p. 1293–1298, doi: 10.1126/science.11539488.

Brzezinski, M.A. and Jones, J.L., 2015, Coupling of the distribution of silicon isotopes to the meridional overturning circulation of the North Atlantic Ocean: Deep Sea Research Part II: Topical Studies in Oceanography, v. 116, p. 79–88, doi: 10.1016/j.dsr2.2014.11.015.

Butterfield, N.J., 2003, Exceptional fossil preservation and the Cambrian Explosion: Integrative and Comparative Biology, v. 43, p. 166–177, doi: 10.1093/icb/43.1.166.

Cai, Y., Cortijo, I., Schiffbauer, J.D., and Hua, H., 2017, Taxonomy of the late Ediacaran index fossil *Cloudina* and a new similar taxon from South China: Precambrian Research, v. 298, p. 146–156, doi: 10.1016/j.precamres.2017.05.016.

Cai, Y., Hua, H., Schiffbauer, J.D., Sun, B., and Yuan, X., 2014, Tube growth patterns and microbial mat-related lifestyles in the Ediacaran fossil *Cloudina*, Gaojiashan Lagerstätte, South China: Gondwana Research, v. 25, p. 1008–1018, doi: 10.1016/j.gr.2012.12.027.

Cai, Y., Hua, H., Xiao, S., Schiffbauer, J.D., and Li, P., 2010, Biostratinomy of the late Ediacaran pyritized Gaojiashan Lagerstätte from southern Shaanxi, South China: importance of event deposits: PALAIOS, v. 25, p. 487–506, doi: 10.2110/palo.2009.p09-133r.

Cai, Y., Hua, H., and Zhang, X., 2013, Tube construction and life mode of the late Ediacaran tubular fossil *Gaojiashania cyclus* from the Gaojiashan Lagerstätte: Precambrian Research, v. 224, p. 255–267, doi: 10.1016/j.precamres.2012.09.022.

Cai, Y., Hua, H., Zhuravlev, A. Yu., Gámez Vintaned, J.A., and Ivantsov, A. Yu., 2011a, Discussion of 'First finds of problematic Ediacaran fossil *Gaojiashania* in Siberia and its origin.': Geological Magazine, v. 148, p. 329–333, doi: 10.1017/S0016756810000749.

Cai, Y., Schiffbauer, J.D., Hua, H., and Xiao, S., 2011b, Morphology and paleoecology of the late Ediacaran tubular fossil *Conotubus hemiannulatus* from the Gaojiashan Lagerstätte of southern Shaanxi Province, South China: Precambrian Research, v. 191, p. 46–57, doi: 10.1016/j.precamres.2011.09.002.

Cai, Y., Schiffbauer, J.D., Hua, H., and Xiao, S., 2012, Preservational modes in the Ediacaran Gaojiashan Lagerstätte: pyritization, aluminosilicification, and carbonaceous compression: Palaeogeography, Palaeoclimatology, Palaeoecology, v. 326–328, p. 109–117, doi: 10.1016/j.palaeo.2012.02.009.

Cai, Y., Xiao, S., Hua, H., and Yuan, X., 2015, New material of the biomineralizing tubular fossil *Sinotubulites* from the late Ediacaran Dengying Formation, South China: Precambrian Research, v. 261, p. 12–24, doi: 10.1016/j.precamres.2015.02.002.

Chai, S., Wu, Y., and Hua, H., 2021, Potential index fossils for the Terminal Stage of the Ediacaran System: Journal of Asian Earth Sciences, v. 218, article 104885, doi: 10.1016/j.jseaes.2021.104885.

Chen, Z., Bengtson, S., Zhou, C.M., Hua, H., and Yue, Z., 2008, Tube structure and original composition of *Sinotubulites*: shelly fossils from the late Neoproterozoic in southern Shaanxi, China: Lethaia, v. 41, p. 37–45, doi: 10.1111/j.1502-3931.2007.00040.x.

Chen, W., Cai, Y., Liang, D., and Wang, X., 2022, Two tubular fossil assemblages from the terminal Ediacaran Dengying Formation in southern Shaanxi Province of South China: Precambrian Research, v. 378, 106–762, doi: 10.1016/j.precamres.2022.106762.

Clapham, M.E. and Narbonne, G.M., 2002, Ediacaran epifaunal tiering: Geology, v. 30, p. 627–630, doi: 10.1130/0091-7613(2002)030<0627:EET>2.0.CO;2.

Cohen, P.A., Bradley, A., Knoll, A.H., Grotzinger, J.P., Jensen, S., Abelson, J., Hand, K., Love, G., Metz, J., and Wilson, J.P., 2009, Tubular compression fossils from the Ediacaran Nama group, Namibia: Journal of Paleontology, v. 83, p. 110–122, doi: 10.1666/09-040R.1.

Corsetti, F.A. and Hagadorn, J.W., 2003, The Precambrian–Cambrian transition in the southern Great Basin, USA: The Sedimentary Record, v. 1, p. 4–8, doi: 10.2110/sedred.2003.1.4.

Cortijo, I., Cai, Y., Hua, H., Schiffbauer, J.D., and Xiao, S., 2015a, Life history and autecology of an Ediacaran index fossil: development and dispersal of *Cloudina*: Gondwana Research, v. 28, p. 419–424, doi: 10.1016/j.gr.2014.05.001.

Cortijo, I., Martí Mus, M., Jensen, S., and Palacios, T., 2010, A new species of *Cloudina* from the terminal Ediacaran of Spain: Precambrian Research, v. 176, p. 1–10, doi: 10.1016/j.precamres.2009.10.010.

Cortijo, I., Martí Mus, M., Jensen, S., and Palacios, T., 2015b, Late Ediacaran skeletal body fossil assemblage from the Navalpino anticline, central Spain: Precambrian Research, v. 267, p. 186–195, doi: 10.1016/j.precamres.2015.06.013.

Darroch, S.A.F., Boag, T.H., Racicot, R.A., Tweedt, S., Mason, S.J., Erwin, D.H., and Laflamme, M., 2016, A mixed Ediacaran-metazoan assemblage from the Zaris Sub-basin, Namibia: Palaeogeography, Palaeoclimatology, Palaeoecology, v. 459, p. 198–208, doi: 10.1016/j.palaeo.2016.07.003.

Darroch, S.A.F., Cribb, A.T., Buatois, L.A., Germs, G.J.B., Kenchington, C.G., Smith, E. F., Mocke, H., O'neil, G.R., Schiffbauer, J.D., Maloney, K.M., Racicot, R.A., Turk, K. A., Gibson, B.M., Almond, J., Koester, B., Boag, T.H., Tweedt, S.M., and Laflamme, M., 2021, The trace fossil record of the Nama Group, Namibia: exploring the terminal Ediacaran roots of the Cambrian explosion: Earth-Science Reviews, v. 212, article 103435, doi: 10.1016/j.earscirev.2020.103435.

Darroch, S.A., Smith, E.F., Nelson, L.L., Craffey, M., Schiffbauer, J.D., and Laflamme, M., 2023, Causes and consequences of end-Ediacaran extinction: an update: Cambridge Prisms: Extinction, v. 1, e15, doi: 10.1017/ext.2023.12.

Deocampo, D.M., 2015, Authigenic clay minerals in lacustrine mudstones: Geological Society of America Special Papers, v. 515, p. 49–64, doi: 10.1130/2015.2515(03).

Droser, M.L. and Gehling, J.G., 2008, Synchronous aggregate growth in an abundant new Ediacaran tubular organism: Science, v. 319, p. 1660–1662, doi: 10.1126/science.1152595.

Droser, M.L., Tarhan, L.G., and Gehling, J.G., 2017, The rise of animals in a changing environment: global ecological innovation in the late Ediacaran: Annual Review of Earth and Planetary Sciences, v. 45, p. 593–617, doi: 10.1146/annurev-earth-063016-015645.

Elliott, D.A., Trusler, P.W., Narbonne, G.M., Vickers-Rich, P., Morton, N., Hall, M., Hoffmann, K.H., and Schneider, G.I., 2016, *Ernietta* from the late Ediacaran Nama Group, Namibia: Journal of Paleontology, v. 90, p. 1017–1026, doi: 10.1017/jpa.2016.94.

Fang, R., Liang, Y., Chen, Y., Liu, F., Hua, H., Holmer, L.E., and Zhang, Z., 2022, Late Ediacaran cavity-dwelling filamentous microorganisms accommodated in a valve-like organism from the uppermost Dengying Formation in eastern Yunnan of South China: Precambrian Research, v. 379, article 106820, doi: 10.1016/j.precamres.2022.106820.

Fitzsimmons, J.N. and Steffen, J.M., 2024, The "net" impact of hydrothermal venting on oceanic elemental inventories: contributions to plume geochemistry from the international GEOTRACES program: Oceanography, v. 37, p. 102–115, doi: 10.5670/oceanog.2024.421.

Fraley, C. and Raftery, A.E., 2007, Bayesian Regularization for Normal Mixture Estimation and Model-Based Clustering: R code module, doi: 10.1007/s00357-007-0004-5.

Gehling, J.G., 1999, Microbial mats in terminal Proterozoic siliciclastics; Ediacaran death masks: PALAIOS, v. 14, p. 40–57, doi: 10.2307/3515360.

Geilert, S., Grasse, P., Doering, K., Wallmann, K., Ehlert, C., Scholz, F., Schmidt, M., and Hensen, C., 2020, Impact of ambient conditions on the Si isotope fractionation in marine pore fluids during early diagenesis: Biogeosciences, v. 17, p. 1745–1763, doi: 10.5194/bg-17-1745-2020.

Germs, G.J.B., 1972, New shelly fossils from Nama Group, South West Africa: American Journal of Science, v. 272, p. 752–761, doi: 10.2475/ajs.272.8.752.

Grant, S.W., 1990, Shell structure and distribution of *Cloudina*, a potential index fossil for the terminal Proterozoic: American Journal of Science, v. 290-A, p. 261–294.

Grasse, P., Closset, I., Jones, J.L., Geilert, S., and Brzezinski, M.A., 2020, Controls on dissolved silicon isotopes along the US GEOTRACES Eastern Pacific Zonal Transect (GP16): Global Biogeochemical Cycles, v. 34, e2020GB006538, doi: 10.1029/2020GB006538.

Grotzinger, J.P., Bowring, S.A., Saylor, B.Z., and Kaufman, A.J., 1995, Biostratigraphic and geochronologic constraints on early animal evolution: Science, v. 270, p. 598–604, doi: 10.1126/science.270.5236.598.

Hagadorn, J.W. and Waggoner, B., 2000, Ediacaran fossils from the southwestern Great Basin, United States: Journal of Paleontology, v. 74, p. 349–359, doi: 10.1017/S0022336000031553.

Hall, C.M.S., Droser, M.L., Gehling, J.G., and Dzaugis, M.E., 2015, Paleoecology of the enigmatic *Tribrachidium*: new data from Ediacaran of South Australia: Precambrian Research, v. 269, p. 183–194, doi: 10.1016/j.precamres.2015.08.009.

Hall, J.G., Smith, E.F., Tamura, N., Fakra, S.C., and Bosak, T., 2020, Preservation of erniettomorph fossils in clay-rich siliciclastic deposits from the Ediacaran Wood Canyon Formation, Nevada: Interface focus, v. 10, article 20200012, doi: 10.1098/rsfs.2020.0012.

Han, S., Löhr, S.C., Abbott, A.N., Baldermann, A., Shields, G.A., Cui, H., Kaufman, A.J., Chen, B., and Yu, B., 2024, Authigenic clay mineral constraints on spatiotemporal evolution of restricted, evaporitic conditions during deposition of the Ediacaran Doushantuo Formation: Earth and Planetary Science Letters, v. 626, article 118524, doi: 10.1038/s41598-021-84433-0.

Han, S., Löhr, S.C., Abbott, A.N., Baldermann, A., Voigt, M., and Yu, B., 2022, Authigenicclay mineral evidence for restricted, evaporitic conditions during the emergence of

the Ediacaran Doushantuo Biota: Communications Earth and Environment, v. 3, p. 165, doi: 10.1038/s43247-022-00495-6.

Hodgin, E.B., Nelson, L.L., Wall, C.J., Barrón-Díaz, A.J., Webb, L.C., Schmitz, M.D., Fike, D.A., Hagadorn, J.W., and Smith, E.F., 2021, A link between rift-related volcanism and end-Ediacaran extinction? Integrated chemostratigraphy, biostratigraphy, and U-Pb geochronology from Sonora, Mexico: Geology, v. 49, p. 115–119, doi: 10.1130/G47972.1.

Hornibrook, E.R.C., 1996, Berthierine from the Lower Cretaceous Clearwater Formation, Alberta, Canada: Clays and Clay Minerals, v. 44, p. 1–21, doi: 10.1346/CCMN.1996.0440101.

Hua, H., Chen, Z., Yuan, X., Zhang, L., and Xiao, S., 2005, Skeletogenesis and asexual reproduction in the earliest biomineralizing animal *Cloudina*: Geology, v. 33, p. 277, doi: 10.1130/G21198.

Hua, H., Chen, Z., and Zhang, L. Y., 2004, *Shaanxilithes* from lower Taozichong Formation, Guizhou Province and its geological and paleobiological significance: Journal of Stratigraphy, v. 28, p. 265–269.

Hua, H., Zhang, L. Y., Zhang, Z. F., and Wang, J.P., 2000, New fossil evidences from latest Neoproterozoic Gaojiashan biota, south Shaanxi: Acta Palaeontologica Sinica, v. 39, p. 381–390.

Isson, T.T. and Planavsky, N.J., 2018, Reverse weathering as a long-term stabilizer of marine pH and planetary climate: Nature, v. 560, p. 471–475, doi: 10.1038/s41586-018-0408-4.

Jensen, S., 2003, The Proterozoic and earliest Cambrian trace fossil record; patterns, problems and perspectives: Integrative and Comparative Biology, v. 43, p. 219–228, doi: 10.1093/icb/43.1.219.

Jensen, S., Droser, M.L., Gehling, J.G., Xiao, S., and Kaufman, A.J., 2006, Neoproterozoic geobiology and paleobiology: Topics in Geobiology, v. 27, p. 115–157.

Joel, L.V., Droser, M.L., and Gehling, J.G., 2014, A new enigmatic, tubular organism from the Ediacara Member, Rawnsley Quartzite, South Australia: Journal of Paleontology, v. 88, p. 253–262, doi: 10.1666/13-058.

Laflamme, M., Darroch, S.A.F., Tweedt, S.M., Peterson, K.J., and Erwin, D.H., 2013, The end of the Ediacara biota: extinction, biotic replacement, or Cheshire Cat?: Gondwana Research, v. 23, p. 558–573, doi: 10.1016/j.gr.2012.11.004.

Laflamme, M., Schiffbauer, J.D., Narbonne, G.M., and Briggs, DE., 2011, Microbial biofilms and the preservation of the Ediacara biota: Lethaia, v. 44, p. 203–213, doi: 10.1111/j.1502-3931.2010.00235.x.

Landing, E., 1994, Precambrian–Cambrian boundary global stratotype ratified and a new perspective of Cambrian time: Geology, v. 22, p. 179, doi: 10.1130/0091-7613(1994)022<0179:PCBGSR>2.3.CO;2.

Maliva, R.G., Knoll, A.H., and Siever, R., 1989, Secular change in chert distribution: a reflection of evolving biological participation in the silica cycle: PALAIOS, v. 4, p. 519, doi: 10.2307/3514743.

Mehra, A. and Maloof, A., 2018, Multiscale approach reveals that *Cloudina* aggregates are detritus and not in situ reef constructions: Proceedings of the National Academy of Sciences, v. 115, doi: 10.1073/pnas.1719911115.

Meyer, M., Schiffbauer, J.D., Xiao, S., Cai, Y., and Hua, H., 2012, Taphonomy of the upper Ediacaran enigmatic ribbonlike fossil *Shaanxilithes*: PALAIOS, v. 27, p. 354–372, doi: 10.2110/palo.2011.p11-098r.

Mitchell, E.G., Kenchington, C.G., Liu, A.G., Matthews, J.J., and Butterfield, N.J., 2015, Reconstructing the reproductive mode of an Ediacaran macro-organism: Nature, v. 524, p. 343–346, doi: 10.1038/nature14646.

Morgan, S.S. and Law, R.D., 1998, An overview of Paleozoic–Mesozoic structures developed in the central White-Inyo Range, Eastern California: International Geology Review, v. 40, p. 245–256, doi: 10.1080/00206819809465208.

Narbonne, G.M., 2005, The Ediacara Biota: Neoproterozoic origin of animals and their ecosystems: Annual Review of Earth and Planetary Sciences, v. 33, p. 421–442, doi: 10.1146/annurev.earth.33.092203.122519.

Narbonne, G.M., Myrow, P.M., Landing, E., and Anderson, M.M., 1987, A candidate stratotype for the Precambrian–Cambrian boundary, Fortune Head, Burin Peninsula, southeastern Newfoundland: Canadian Journal of Earth Sciences, v. 24, p. 1277–1293, doi: 10.1139/e87-124.

Narbonne, G.M., Xiao, S., Shields, G.A., and Gehling, J.G., 2012, The Ediacaran Period: The Geologic Time Scale, v. 1, p. 413–435.

Nelson, C.A., 1962, Lower Cambrian–Precambrian succession, White Inyo Mountains, California: Geological Society of America Bulletin, v. 73, p. 139, doi: 10.1130/0016-7606(1962)73[139:LCSWMC]2.0.CO;2.

Nelson, L.L., Crowley, J.L., Smith, E.F., Schwartz, D.M., Hodgin, E.B., and Schmitz, M. D., 2023, Cambrian explosion condensed: high-precision geochronology of the lower Wood Canyon Formation, Nevada: Proceedings of the National Academy of Sciences, v. 120, e2301478120, doi: 10.1073/pnas.2301478120.

Penny, A.M., Wood, R., Curtis, A., Bowyer, F., Tostevin, R., and Hoffman, K.H., 2014, Ediacaran metazoan reefs from the Nama Group, Namibia: Science, v. 344, p. 1504–1506, doi: 10.1126/science.1253393.

Pruss, S.B., Smith, E.F., Leadbetter, O., Nolan, R.Z., Hicks, M., and Fike, D.A., 2019, Palaeoecology of the archaeocyathan reefs from the lower Cambrian Harkless Formation, southern Nevada, western United States and carbon isotopic evidence for their demise: Palaeogeography, Palaeoclimatology, Palaeoecology, v. 536, article 109389, doi: 10.1016/j.palaeo.2019.109389.

Raiswell, R., Whaler, K., Dean, S., Coleman, M.L., and Briggs, D.E.G., 1993, A simple three-dimensional model of diffusion-with-precipitation applied to localised pyrite formation in framboids, fossils, and detrital iron minerals: Marine Geology, v. 113, p. 89–100, doi: 10.1016/0025-3227(93)90151-K.

Rogov, V., Marusin, V., Bykova, N., Goy, Y., Nagovitsin K., Kochnev, B., Karlova, G., and Grazhdankin, D., 2012, The oldest evidence of bioturbation on Earth: Geology, v. 40, p. 395–398, doi: 10.1130/G32807.1.

Sappenfield, A., Droser, M.L., and Gehling, J.G., 2011, Problematica, trace fossils, and tubes within the Ediacara Member (South Australia): redefining the Ediacaran trace fossil record one tube at a time: Journal of Paleontology, v. 85, p. 256–265, doi: 10.1666/10-068.1.

Schiffbauer, J.D., Huntley, J.W., O'Neil, G.R., Darroch, S.A.F., Laflamme, M., and Cai, Y., 2016, The latest Ediacaran wormworld fauna: setting the ecological stage for the Cambrian Explosion: GSA Today, v. 26, p. 4–11, doi: 10.1130/GSATG265A.1.

Schiffbauer, J.D., Selly, T., Jacquet, S.M., Merz, R.A., Nelson, L.L., Strange, M.A., Cai, Y., and Smith, E.F., 2020, Discovery of bilaterian-type through-guts in cloudinomorphs from the terminal Ediacaran Period: Nature Communications, v. 11, p. 205, doi: 10.1038/s41467-019-13882-z.

Seilacher, A., 1989, Vendozoa: organismic construction in the Proterozoic biosphere: Lethaia, 22, p. 229–239, doi: 10.1111/j.1502-3931.1989.tb01332.x.

Seilacher, A., Buatois, L.A., and Gabriela Mángano, M., 2005, Trace fossils in the Ediacaran–Cambrian transition: behavioral diversification, ecological turnover and environmental shift: Palaeogeography, Palaeoclimatology, Palaeoecology, v. 227, p. 323–356, doi: 10.1016/j.palaeo.2005.06.003.

Seilacher, A., Reif, W.E., and Westphal, F., 1985, Sedimentological, ecological and temporal patterns of fossil Lagerstätten: Philosophical Transactions of the Royal Society of London B, Biological Sciences, v. 311, p. 5–24, doi: 10.1098/rstb.1985.0134.

Selly, T., Schiffbauer, J.D., Jacquet, S.M., Smith, E.F., Nelson, L.L., Andreasen, B.D., Huntley, J.W., Strange, M.A., O'Neil, G.R., Thater, C.A., Bykova, N., Steiner, M., Yang, B., and Cai, Y., 2020, A new cloudinid fossil assemblage from the terminal Ediacaran of Nevada, USA: Journal of Systematic Palaeontology, v. 18, p. 357–379, doi: 10.1080/14772019.2019.1623333.

Shen, B., Xiao, S., Dong, L., Chuanming, Z., and Liu, J., 2007, Problematic macrofossils from Ediacaran successions in the North China and Chaidam blocks: implications for their evolutionary roots and biostratigraphic significance: Journal of Paleontology, v. 81, p. 1396–1411, doi: 10.1666/06-016R.1.

Siever, R., 1992, The silica cycle in the Precambrian: Geochimica et Cosmochimica Acta, v. 56, p. 3265–3272, doi: 10.1016/0016-7037(92)90303-Z.

Signor, P.W., Mount, J.F., and Onken, B.R., 1987, A pre-trilobite shelly fauna from the White–Inyo region of eastern California and western Nevada: Journal of Paleontology, v. 61, p. 425–438, doi: 10.1017/S0022336000028614.

Slagter, S., Konhauser, K.O., Briggs, D.E.G., and Tarhan, L.G., 2024a, Controls on authigenic mineralization in experimental Ediacara-style preservation: Geobiology, v. 22, e12615, doi: 10.1111/gbi.12615.

Slagter, S., Tarhan, L.G., Blum, T.B., Droser, M.L., and Valley, J.W., 2024b, Silica cementation history of the Ediacara Member (Rawnsley Quartzite, South Australia): insights from petrographic and *in situ* oxygen isotopic microanalyses: Precambrian Research, v. 402, article 107288, doi: 10.1016/j.precamres.2024.107288.

Smith, E.F., Nelson, L.L., O'connell, N., Eyster, A., and Lonsdale, M.C., 2023, The Ediacaran−Cambrian transition in the southern Great Basin, United States: GSA Bulletin, v. 135, p. 1393–1414, doi: 10.1130/B36401.

Smith, E.F., Nelson, LL., Strange, M. A., Eyster, A.E., Rowland, S.M., Schrag, D.P., and MacDonald, F.A., 2016, The end of the Ediacaran: two new exceptionally preserved body fossil assemblages from Mount Dunfee, Nevada, USA: Geology, v. 44, p. 911–914, doi: 10.1130/G38157.1.

Smith, E.F., Nelson, L.L., Tweedt, SM., Zeng, H., and Workman, J.B., 2017, A cosmopolitan late Ediacaran biotic assemblage: new fossils from Nevada and Namibia support a global biostratigraphic link: Proceedings of the Royal Society B, Biological Sciences, v. 284, article 20170934, doi: 10.1098/rspb.2017.0934.

Sour-Tovar, F., Hagadorn, J.W., and Huitrón-Rubio, T., 2007, Ediacaran and Cambrian index fossils from Sonora, Mexico: Palaeontology, v. 50, p. 169–175, doi: 10.1111/j.1475-4983.2006.00619.x.

Sperling, E.A., Wolock, C.J., Morgan, A.S., Gill, B.C., Kunzmann, M., Halverson, G.P., MacDonald, F.A., Knoll, A.H., and Johnston, D.T., 2015, Statistical analysis of iron geochemical data suggests limited late Proterozoic oxygenation: Nature, v. 523, p. 451–454, doi: 10.1038/nature14589.

Stewart, J.H., 1970, Upper Precambrian and lower Cambrian strata in the southern Great Basin California and Nevada: USGS Professional Paper 620, 206 p., doi: 10.3133/pp620.

Stewart, J.H., Ross, D.C., Nelson, C.A., and Burchfiel, B.C., 1966, Last Chance thrust—a major fault in the eastern part of Inyo County, California: USGS Professional Paper 550D, p. D23–D34.

Surprenant, R.L., Gehling, J.G., and Droser, M.L., 2020, Biological and ecological insights from the preservational variability of *Funisia dorothea*, Ediacara Member, South Australia: PALAIOS, v. 35, p. 359–376, doi: 10.2110/palo.2020.014.

Surprenant, R.L. and Droser, M.L., 2024, New insight into the global record of the Ediacaran tubular morphotype: a common solution to early multicellularity: Royal Society Open Science, v. 11, p. 231–313, doi: 10.1098/rsos.231313.

Tarhan, L.G., Droser, M.L., Cole, D.B., and Gehling, J.G., 2018, Ecological expansion and extinction in the late Ediacaran: weighing the evidence for environmental and biotic drivers: Integrative and Comparative Biology, v. 58, p. 688–702, doi: 10.1093/icb/icy020.

Tarhan, L.G., Hood, A.V.S., Droser, M.L., Gehling, J.G., and Briggs, D.E.G., 2016, Exceptional preservation of soft-bodied Ediacara Biota promoted by silica-rich oceans: Geology, v. 44, p. 951–954, doi: 10.1130/G38542.1.

Tarhan, L.G., Hughes, N.C., Myrow, P.M., Bhargava, O.N., Ahluwalia, A.D., and Kudryavtsev, A.B., 2014, Precambrian–Cambrian boundary interval occurrence and form of the enigmatic tubular body fossil *Shaanxilithes ningqiangensis* from the Lesser Himalaya of India: Palaeontology, v. 57, p. 283–298, doi: 10.1111/pala.12066.

Tarhan, L G., Myrow, P.M., Smith, E.F., Nelson, L.L., and Sadler, P.M., 2020, Infaunal augurs of the Cambrian explosion: an Ediacaran trace fossil assemblage from Nevada, USA: Geobiology, v. 18, p. 486–496, doi: 10.1111/gbi.12387.

Trower, E.J. and Fischer, W.W., 2019, Precambrian Si isotope mass balance, weathering, and the significance of the authigenic clay silica sink: Sedimentary Geology, v. 384, p. 1–11, doi: 10.1016/j.sedgeo.2019.02.008.

Turk, K.A., Maloney, K.M., Laflamme, M., and Darroch, S.A.F., 2022, Paleontology and ichnology of the late Ediacaran Nasep–Huns transition (Nama Group, southern Namibia): Journal of Paleontology, v. 96, p. 753–769, doi: 10.1017/jpa.2022.31.

Vinn, O. and Zaton, M., 2012, Inconsistencies in proposed annelid affinities of early biomineralized organism *Cloudina* (Ediacaran): structural and ontogenetic evidences: Carnets Géol, v. 3, p. 39–47, doi: 10.4267/2042/46095.

Wade, M., 1968, Preservation of soft-bodied animals in Precambrian sandstones at Ediacara, South Australia: Lethaia, v. 1, p. 238–267.

Wang, X., Zhang, X., and Liu, W., 2021, Biostratigraphic constraints on the age of Neoproterozoic glaciation in North China: Journal of Asian Earth Sciences, v. 219, p. 104–894, doi: 10.1016/j.jseaes.2021.104894.

Weber, B., Steiner, M., and Zhu, M.-Y., 2007, Precambrian–Cambrian trace fossils from the Yangtze Platform (South China) and the early evolution of bilaterian lifestyles: Palaeogeography, Palaeoclimatology, Palaeoecology, v. 254, p. 328–349, doi: 10.1016/j.palaeo.2007.03.021.

Wernicke, B., Axen, G.J., and Snow, J. K., 1988, Basin and Range extensional tectonics at the latitude of Las Vegas, Nevada: Geological Society of America Bulletin, v. 100, p. 1738–1757, doi: 10.1130/0016-7606(1988)100<1738:BARETA>2.3.CO;2.

Wood, R., 2018, Exploring the drivers of early biomineralization: Emerging Topics in Life Sciences, v. 2, p. 201–212, doi: 10.1042/ETLS20170164.

Wood, R., Curtis, A., Penny, A., Zhuravlev, A. Yu., Curtis-Walcott, S., Iipinge, S., and Bowyer, F., 2017, Flexible and responsive growth strategy of the Ediacaran skeletal *Cloudina* from the Nama Group, Namibia: Geology, v. 45, p. 259–262, doi: 10.1130/G38807.1.

Xiao, S. and Laflamme, M., 2009, On the eve of animal radiation: phylogeny, ecology and evolution of the Ediacara biota: Trends in Ecology and Evolution, v. 24, p. 31–40, doi: 10.1016/j.tree.2008.07.015.

Xiao, S., Narbonne, G.M., Zhou, C., Laflamme, M., Grazhdankin, D.V., Moczydlowska-Vidal, M., and Cui, H., 2016, Towards an Ediacaran time scale: problems, protocols, and prospects: Episodes Journal of International Geoscience, v. 39, p. 540–555, doi: 10.18814/epiiugs/2016/v39i4/103886.

Yang, B., Steiner, M., Schiffbauer, J.D., Selly, T., Wu, X., Zhang, C., and Liu, P., 2020, Ultrastructure of Ediacaran cloudinids suggests diverse taphonomic histories and affinities with non-biomineralized annelids: Scientific Reports, v. 10, p. 535, doi: 10.1038/s41598-019-56317-x.

Yang, B., Warren, L.V., Steiner, M., Smith, E.F., and Liu, P., 2022, Taxonomic revision of Ediacaran tubular fossils: *Cloudina*, *Sinotubulites* and *Conotubus*: Journal of Paleontology, v. 96, p. 256–273, doi: 10.1017/jpa.2021.95.

Yue, Z., Bengtson, S., and Grant, S.W.F., 1992, Biology and functional morphology of *Cloudina*, the earliest known metazoan with a mineralized skeleton: The Paleontological Society Special Publications, v. 6, p. 325–325, doi: 10.1017/S2475262200008856.

Zhang, L., Ding, L., Li, Y., and Dong, J., 1992, The study of the late Sinian–early Cambrian biotas from the northern margin of the Yangtze Platform: Scientific and Technical Documents Publishing House, Beijing, v. 135.

Zhuravlev, A. Yu., Vintaned, J.A.G., and Ivantsov, A. Yu., 2009, First finds of problematic Ediacaran fossil *Gaojiashania* in Siberia and its origin: Geological Magazine, v. 146, p. 775–780, doi: 10.1017/S0016756809990185.

Received 20 March 2024; accepted 25 September 2024.